H_2-IGCC Project Deliverable

Grant Agreement number	239349
Project acronym	H_2-IGCC
Project title	Low Emission Gas Turbine Technology for Hydrogen-rich Syngas
Funding Scheme	FP7-ENERGY-2008-TREN-1
Subproject	**SP2 – Materials**
Work Package	**WP2.2 – Performance of state-of-the-art materials/coatings in novel operating conditions**
Deliverable number – title	**D2.2.2 – Report on high temperature oxidation, thermal cycling and corrosion of TBCs (including blade, vane and combustor variants) in combusted syngas environments (includes lab and burner rig exposures)**
Lead Beneficiary	**Forschungszentrum Jülich**
Dissemination Level	**Confidential**
Delivery Month	**M44**
Name, title and organisation of the scientific representative of the project's coordinator	Christer Björkqvist Managing Director, European Turbine Network (ETN) Tel: 00 32 2 646 1577 Fax: 00 32 2 646 1578 E-mail: cb@etn-gasturbine.eu Project website address: www.h2-igcc.eu

Report
on high temperature oxidation, thermal cycling and corrosion
of state-of-the-art TBCs
(including blade, vane and combustor variants)
in combusted syngas environments
(includes lab and burner rig exposures)

Deliverable 2.2.2

SEVENTH FRAMEWORK PROGRAMME
FP7-ENERGY-2008-TREN-1
ENERGY-2008-6-CLEAN COAL TECHNOLOGIES
Project Acronym: H2-IGCC
Project Full Title: Low Emission Gas Turbine Technology for Hydrogen-rich Syngas
Grant Agreement No.: 239349
SP2: Materials

Daniel E. Mack*, Dmitry Naumenko, Maria O. Jarligo, Wojciech Nowak
(* corresponding)

Revisions history

Revision number	Date	List of modifications
0	2013-06-21	First emission

Contents

Foreword

The overall objective of the H2-IGCC project is to provide and demonstrate technical solutions which will allow the use of state-of-the-art highly efficient, reliable gas turbines (GTs) in the next generation of Integrated Gasification Combined Cycle (IGCC) plants. The goal is to enable combustion of undiluted hydrogen-rich syngas with low NOx emissions and also allowing for high fuel flexibility. The challenge is to operate a stable and controllable GT on hydrogen-rich syngas with emissions and processes similar to current state-of-the-art natural GT engines. The H2-IGCC project aims to tackle this challenge as well as fuel flexibility, by enabling the burning of back-up fuels, such as natural gas, without adversely affecting the reliability and availability.

The technical challenges being addressed by the H2-IGCC project are divided into 4 Subprojects (SP):

- COMBUSTION (SP1)
- MATERIALS (SP2)
- TURBOMACHINERY (SP3)
- SYSTEM ANALYSIS (SP4)

SP2 deals with improved materials systems with advanced coatings able to protect hot path components base materials against different temperatures and compositions of exhaust gases. Cost-effective materials and coatings technologies will be developed to overcome the component life-limiting problems of overheating and of hot corrosion resulting from the higher temperatures and residual contaminants in the syngas, including validation of materials performance data, life prediction and monitoring methods. Simulation tools for estimating performance and lifetime of materials systems will also be enhanced to suit the new operating environments.

Forschungszentrum Jülich is involved in SP2 within several Work Packages. This report covers results from activities on performance of TBC coated materials from several tasks within work package 2.2 (Performance of state-of-the-art materials/coatings in novel operating conditions):

- T2.2.2: High temperature oxidation and thermal cycling
- T2.2.3: High temperature corrosion (CMAS interactions)
- T2.2.7: Burner rig exposures
- T2.2.8: Detailed microstructural characterisation

In particular, activities on T2.2.8 are still on-going and interpretation preliminary. Final summary will be included to new established deliverable D2.2.8.

High-Temperature Oxidation, Thermal Cycling Tests

Experimental

Coating systems

Cycling oxidation exposures were performed with the state of the art air plasma sprayed (APS) thermal barrier coating (TBC) systems based on Rene 80 superalloy and with bondcoats (BC) of the types SC-2464 and SC-2231, which were produced by Flamespray (FS) and Forschungszentrum Jülich (FZJ). The specimen geometry is shown in Figure 1. The bondcoats were sprayed using high velocity oxyfuel (HVOF) facility available at Flamespray and vacuum plasma spraying facility (VPS) available at FZJ. After bondcoat spraying the samples were heat-treated in vacuum according to the specification for Rene 80. The thermal barrier coatings based on partially yttria stabilized zirconia (YSZ; 6-8%Y2O3-ZrO2) were sprayed by APS at FS and FZJ.

Test conditions

The first set of the oxidation tests was performed at 1050°C with 100 h cycles in resistance heated tube furnaces. The test gases were synthetic air and synthetic air with addition of 20% H2O. The water vapour content in the second gas was set up using bubble humidifier. The heating and cooling of the samples was performed in the test gases. The specimens were inspected for TBC-failure during cooling intervals, i.e. each 100 hours. The failure criterion was an edge crack in the TBC of a minimum length of 5 mm. Two specimens of each batch were exposed till failure to check the lifetime reproducibility. In order to study the effect of atmosphere on the formation of the thermally grown oxide (TGO), additional specimens were exposed up to 100 hours (one cycle, i.e. isothermal exposure). After finishing the tests, metallographic cross-sections were prepared from the oxidized samples and the samples in the as-received conditions. The cross-sections were investigated using optical metallography and scanning electron microscopy (SEM).

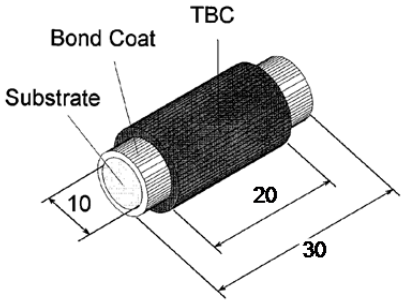

Figure 1 Nominal geometry of TBC-specimens (in mm) used for cyclic oxidation testing

The second set of experiments with the above TBC systems and under the same atmospheres and cyclic conditions has been initiated at 950°C with some delay due to a late coating delivery. The test times are 100 h and 1000 h, i.e. no TBC-lifetime data are being generated. Therefore these tests are not considered to be critical for the current deliverable. After completing the tests the same procedure will be used for the materials characterization as after the 1050°C tests. The results of the tests and analytical studies will be available in about 6 months.

The table on the following page gives an overview of the systems produced and experimental conditions used for testing under cyclic oxidation.

Table 1: Overview of TBC systems produced, experimental conditions for testing and test status

Coating System	Coating facility	Test Times	No. of samples	Temp., °C	Test status	Test Environ-ments
SC-2464 (VPS) + TBC (APS) (batch name: NOF)	FZJ	0h, 100 h, x2 End of Life	4	1050	completed	Synth. air, Synth. air + 20% H_2O
SC-2464 (HVOF) + TBC (APS) (batch name: NOG)	Flamespray (BC) + FZJ (TBC)	0h, 100 h, x2 End of Life	4			
SC-2464 (HVOF) + TBC (APS) (batch name: NLK)	Flamespray	0h, 100 h, x2 End of Life	4			
SC-2231 (HVOF) + TBC (APS) (batch name: NOL)	Flamespray	0h, 100 h, x2 End of Life	4			
SC-2464 (VPS) + TBC (APS) (batch name: NOF)	FZJ	100 h, 1000 h	2	950	on-going	
SC-2464 (HVOF) + TBC (APS) (batch name: NLK)	Flamespray	100 h, 1000 h	2			
SC-2231 (HVOF) + TBC (APS) (batch name: NOL)	Flamespray	100 h, 1000 h	2			

Results

Figure 2 shows metallographic cross-sections of the studied TBC-systems in the as-received conditions. The systems with HVOF bondcoat have a clearly different bondcoat roughness profile compared to the VPS bondcoat. In addition it is obvious that the TBC-systems produced at Flamespray feature a more porous topcoat than the systems produced at FZJ.

Figure 3 shows lifetime barcharts of the studied TBC systems. It can be seen that there are lifetime variations between various systems as well as for some of the systems between the exposures in dry and wet atmospheres. The lifetime of the TBC systems with SC-2464 HVOF bondcoat and TBC from FS (Batch NLK) in both synthetic (dry) and wet air at 1050°C is about 1500 hours with very good reproducibility. In contrast the system with the same bondcoat but TBC from FZJ (Batch NOG) has much shorter, reproducible lifetimes in the wet (around 900 hours) than in the dry (about 1500 hours) test gas. A similar trend of reduced TBC-lifetime in the wet gas might also be present with the complete TBC system produced at FZJ (Batch NOF), with nominally the same BC and TBC compositions as NLK and NOG. In the dry gas, however, the lifetime reproducibility was not very good, which prevents a definite conclusion on the effect of water vapour for the system NOF. Finally, the system by FS with SC-2231 exhibits in both test gases an about 30% longer lifetime than the system with SC-2464 bondcoat. In order to elucidate the reasons for the observed lifetime variations extensive analytical studies were performed as summarized below.

Figure 4 and Figure 5 show macro-images of the failed specimens. It can be seen that the failure modes are very similar in all cases, i.e. in all studied systems and in both atmospheres, namely crack initiation at the TBC edge, which propagates towards the sample centre.

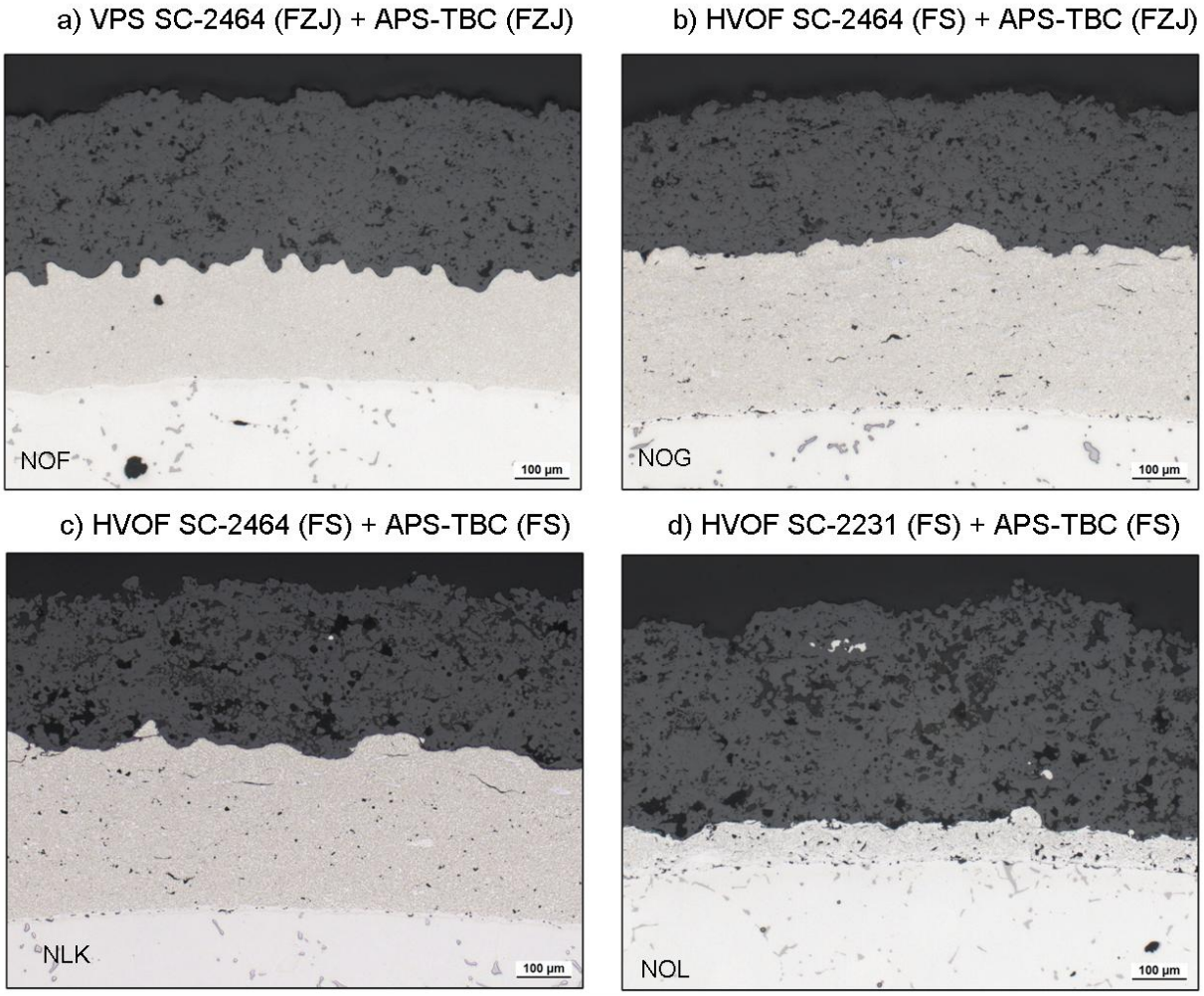

Figure 2: Metallographic cross-sections of the studied TBC-systems in the as-received conditions

Figure 6 to Figure 9show metallographic cross-sections of the studied TBC-systems after 100 h exposure at 1050°C comparing the two test atmospheres. One system (batch NOG), which was macroscopically intact after 100 h exposure in synthetic air failed during the sample preparation and a large gap was found propagating in the TBC close to the TBC/BC interface (Figure 7). From Figure 6 to Figure 9 it is, however, clear that the initial TGO-morphologies are very similar in the two atmospheres studied.

Figure 10-Figure 13 and Figure 14-Figure 15 show the optical metallographic and SEM cross-sections respectively of the studied systems after macroscopic TBC-failure. For a given system the failure modes are very similar between the samples exposed to dry and wet gases in agreement with the macro-images of the failed specimens presented in Figure 4 and Figure 5. The lifetime data in Figure 3 indicate that the for the majority of the TBC-systems the lifetime is not affected by the presence of water vapour. An exception is the TBC system with HVOF SC-2464 bondcoat and dense topcoat (batch NOG), for which the lifetime is significantly shorter in dry than in wet air. Unfortunately the metallographic (Figure 11) and SEM (Figure 15) analytical examinations in cross-sections do not reveal obvious reasons for these differences.

In both atmospheres the crack propagation paths and TGO-morphologies are very similar. The TGO-thicknesses look also similar, which first seems to be an unexpected result considering the lifetime differences of almost a factor of two. It should be noted, however,

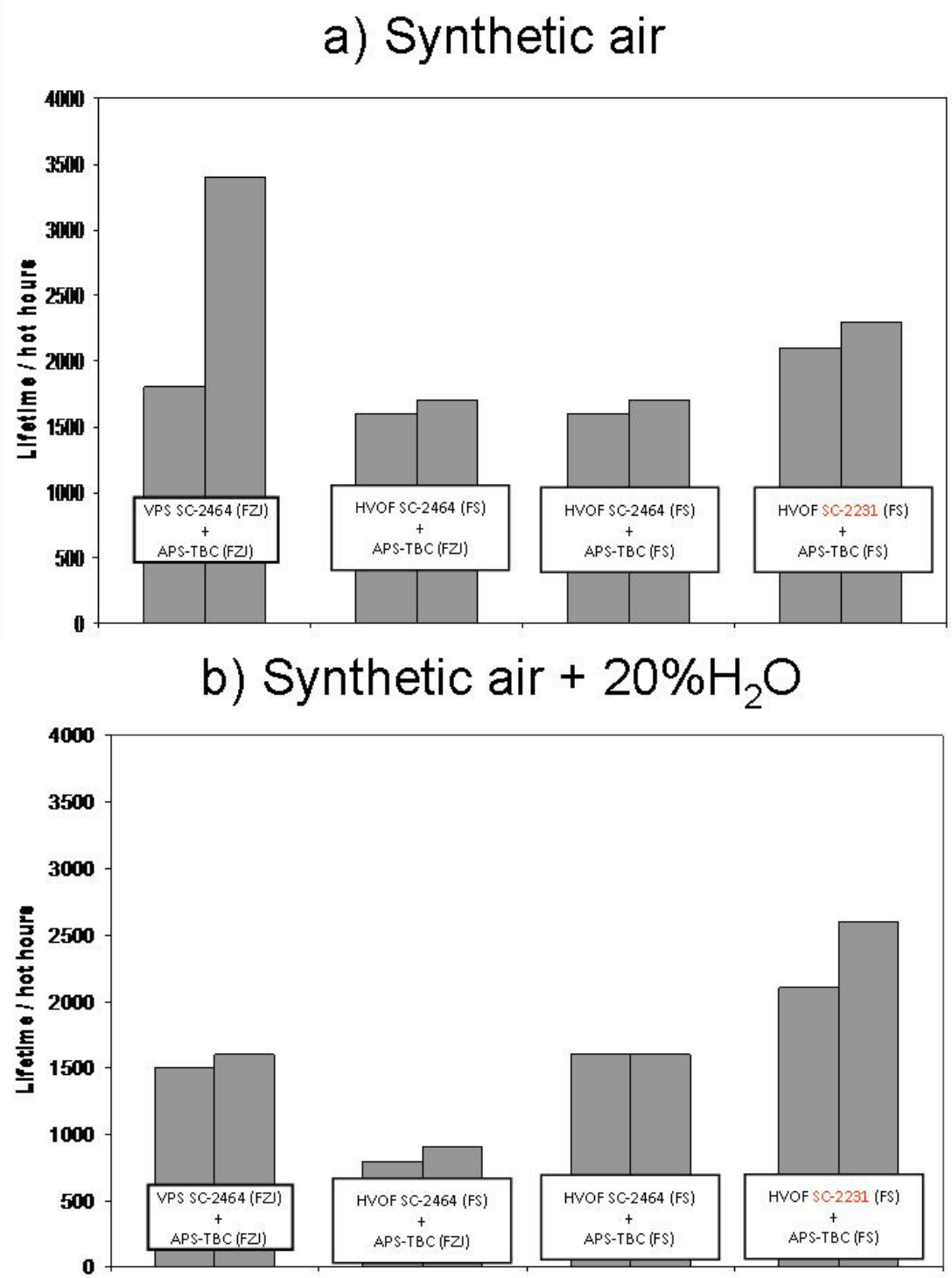

Figure 3: Lifetimes of studied TBC systems during 100 h cycles oxidation at 1050°C in: a) synthetic air and b) synthetic air + 20% H_2O

that intrinsic growth rates of alumina based TGO's found in studies on free-standing coatings (see the report on the oxidation of metallic materials) are in both atmospheres very

similarand sub-parabolic (near cubic). Therefore, the factor of 1600/900≈1.8 difference in exposure time assuming cubic oxidation kinetics should result in TGO thickness difference of only 1.2. Furthermore, from Figure 15 it is obvious that the TGO-thickness is not uniform over the topcoat/bondcoat interface and exhibits in both cases substantial variations. One of the reasons for these variations is the effect of repeated TGO cracking, typically found in the convex regions of the bondcoat surface profile. Considering all the available data it can be concluded that the TGO-formation is not likely to be very much different between the two atmospheres.

Summary and Discussion

Based on the presently available results it can be speculated that the difference in the lifetime of the TBC system NOG (HVOF BC + dense TBC) between the wet and dry atmospheres can be related to the combination of two factors, namely a relatively flat bondcoat and a relatively dense topcoat of this system. This idea is indirectly supported by: a) the fact that a similar but less pronounced tendency of a decreased TBC lifetime was observed in the system NOF (VPS bondcoat and the same topcoat as in NOG) and b) by the fact that the lifetimes of the other two studied TBC systems with HVOF bondcoats (NLK and NOL), which have a more porous topcoat were not found to be affected by the presence of water vapour in the test gas. The possible mechanisms of the effect of water vapour on the lifetime of TBC system NOG are being elucidated in on-going additional studies. These studies include testing for intermediate exposure times to follow the crack initiation and propagation in wet and dry atmospheres. In order to separate better the effects of TBC and BC microstructure on the lifetime of the TBC systems an additional TBC system was produced which has a rough VPS bondcoat and a porous ceramic topcoat. The results of the studies with the new and existing will be presented at the next project meetings.

Finally it should be stressed once again that for the majority of the state of the art TBC systems with optimized TBC porosity the lifetimes measured in the cyclic oxidation tests were not found to be affected by the presence of water vapour in the test gas.

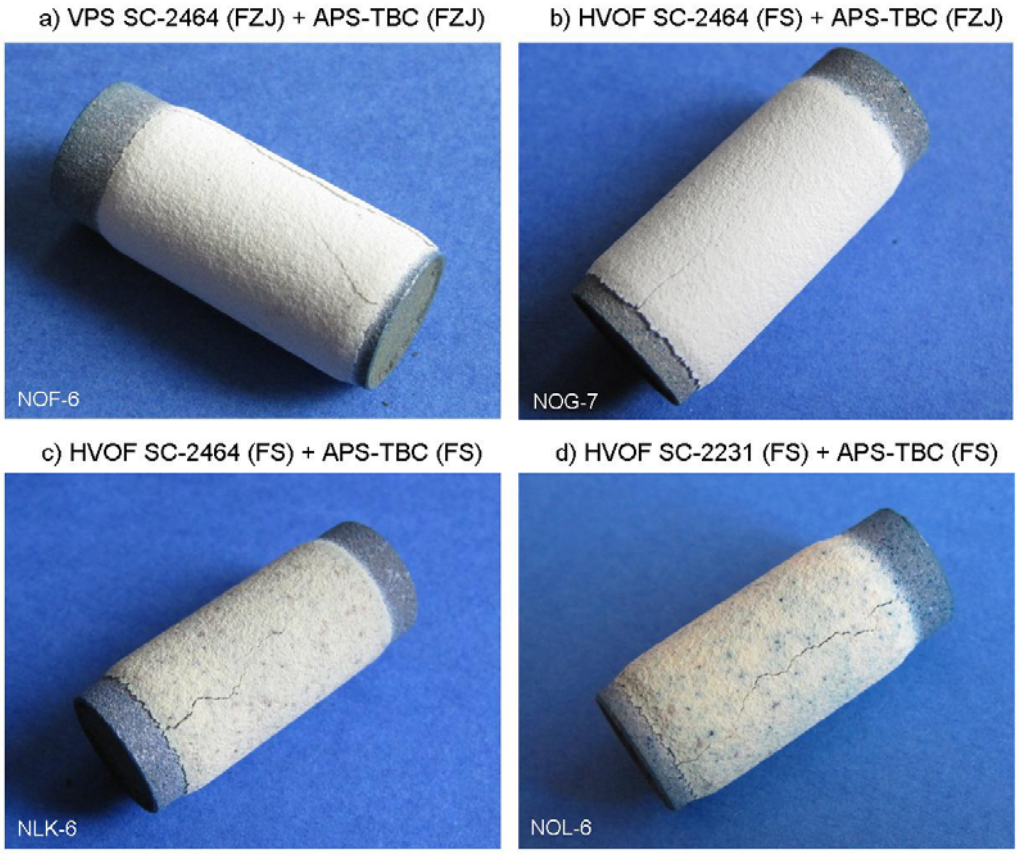

Figure 4: Macro-images of the failed specimens oxidized in synthetic air

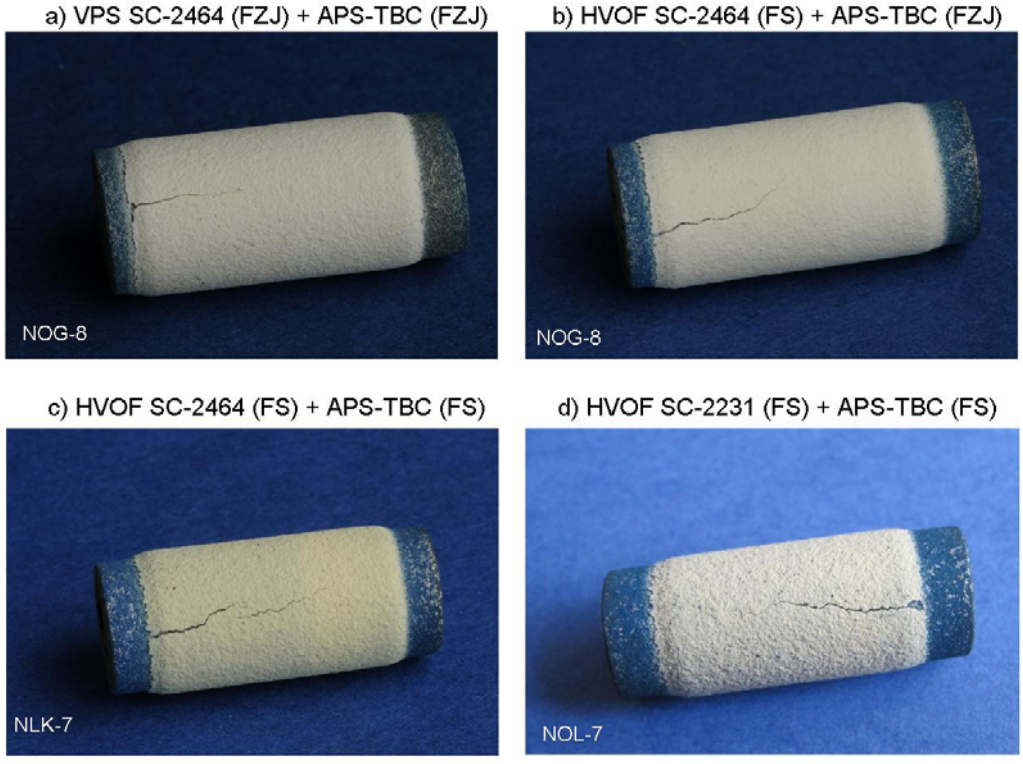

Figure 5: Macro-images of the failed specimens oxidized in synthetic air + 20%H_2O

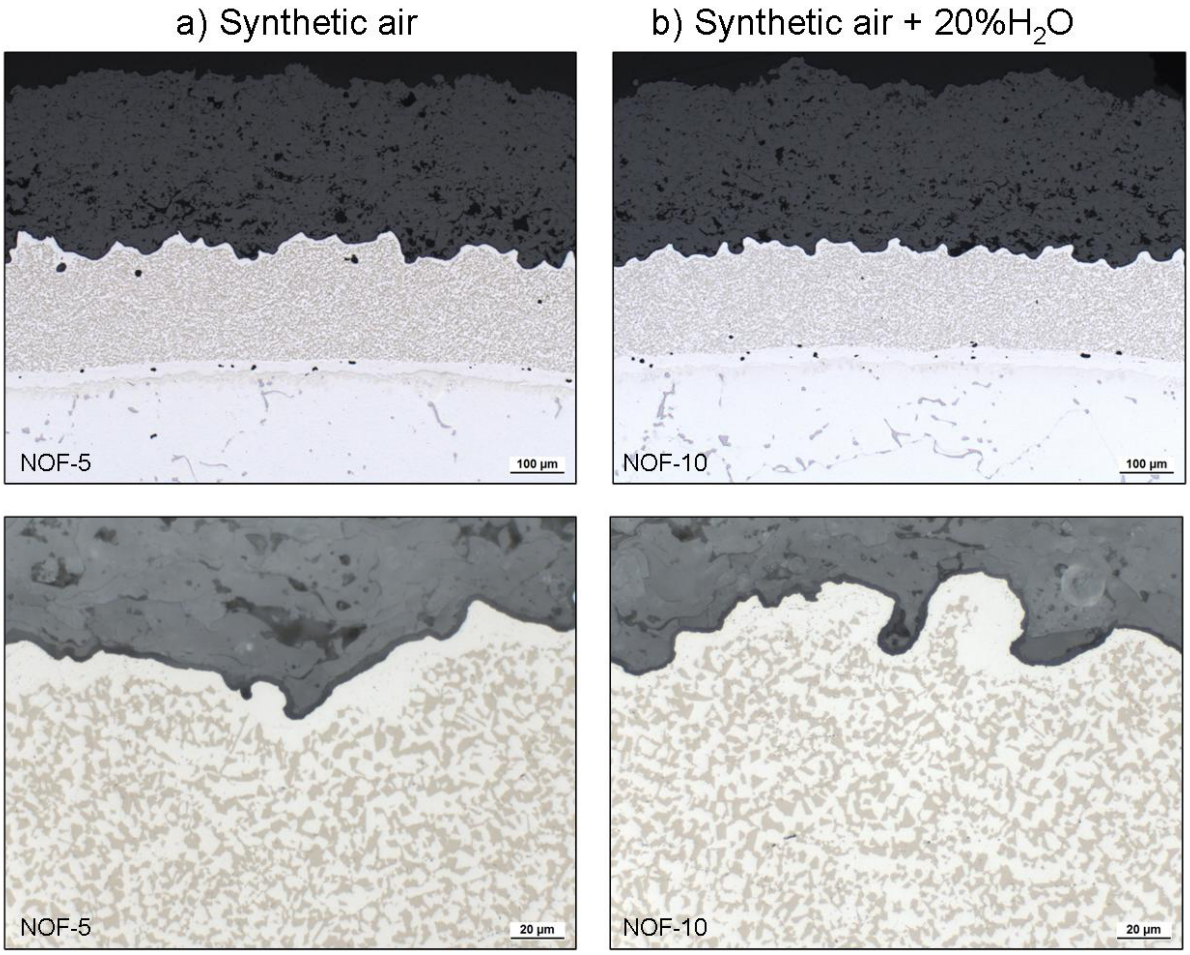

Figure 6 Metallographic cross-sections of the TBC-system NOF : VPS SC-2464 (FZJ) + APS-TBC (FZJ) after 100 h exposure at 1050°C in: a) synthetic air, b) synthetic air + 20%H_2O

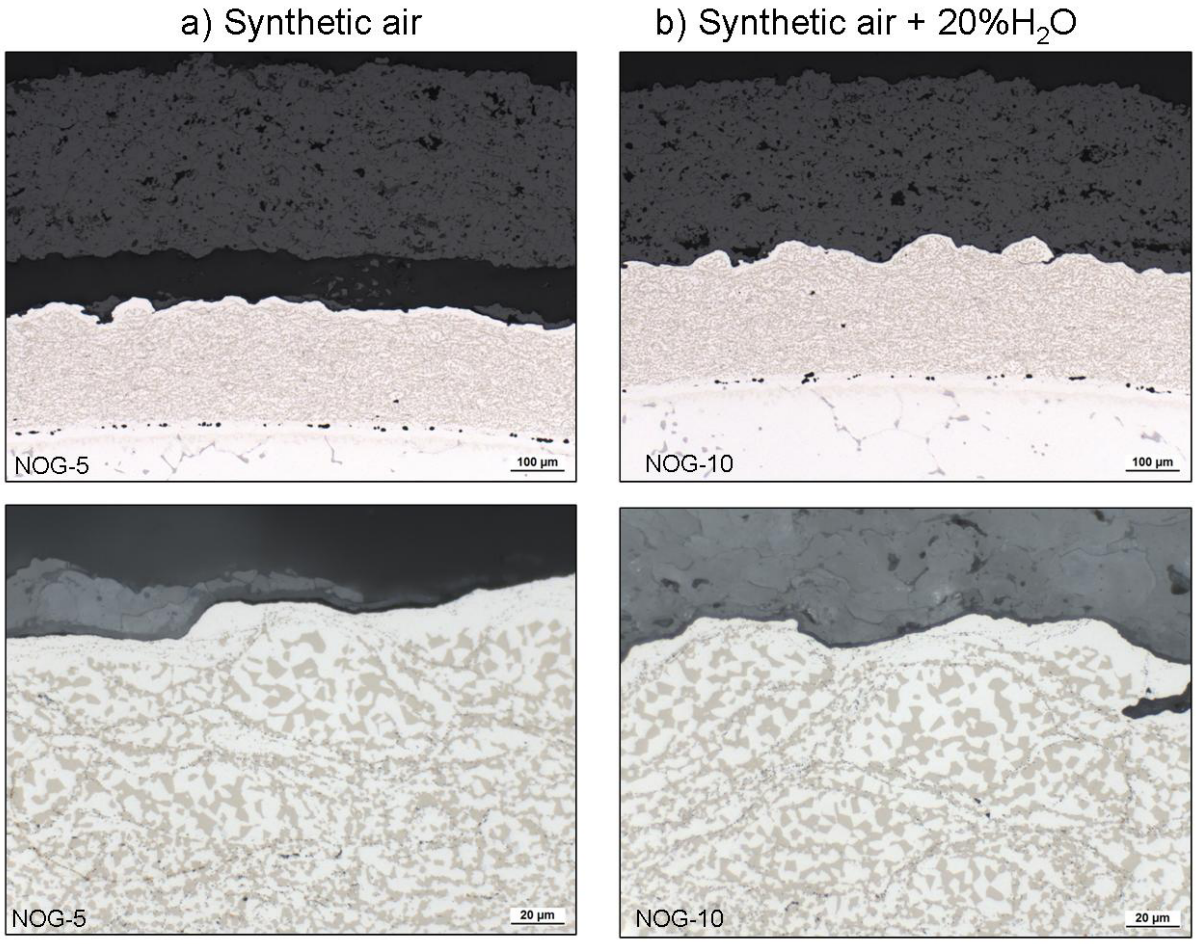

Figure 7: Metallographic cross-sections of the TBC-system NOG: HVOF SC-2464 (FS) + APS-TBC (FZJ) after 100 h exposure at 1050°C in: a) Synthetic air, b) Synthetic air + 20%H_2O

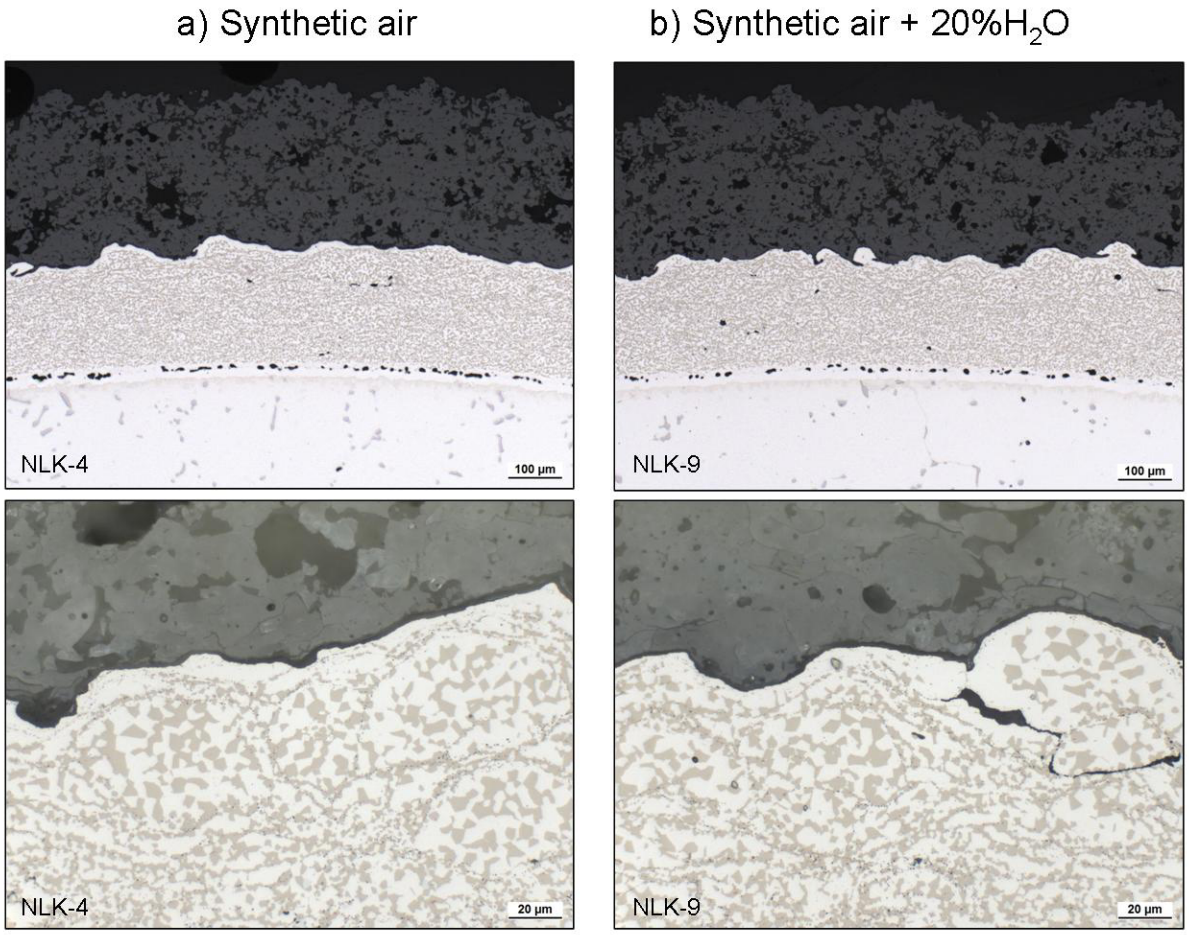

Figure 8: Metallographic cross-sections of the TBC-system NLK: HVOF SC-2464 (FS) + APS-TBC (FS) after 100 h exposure at 1050°C in: a) Synthetic air, b) Synthetic air + 20%H_2O

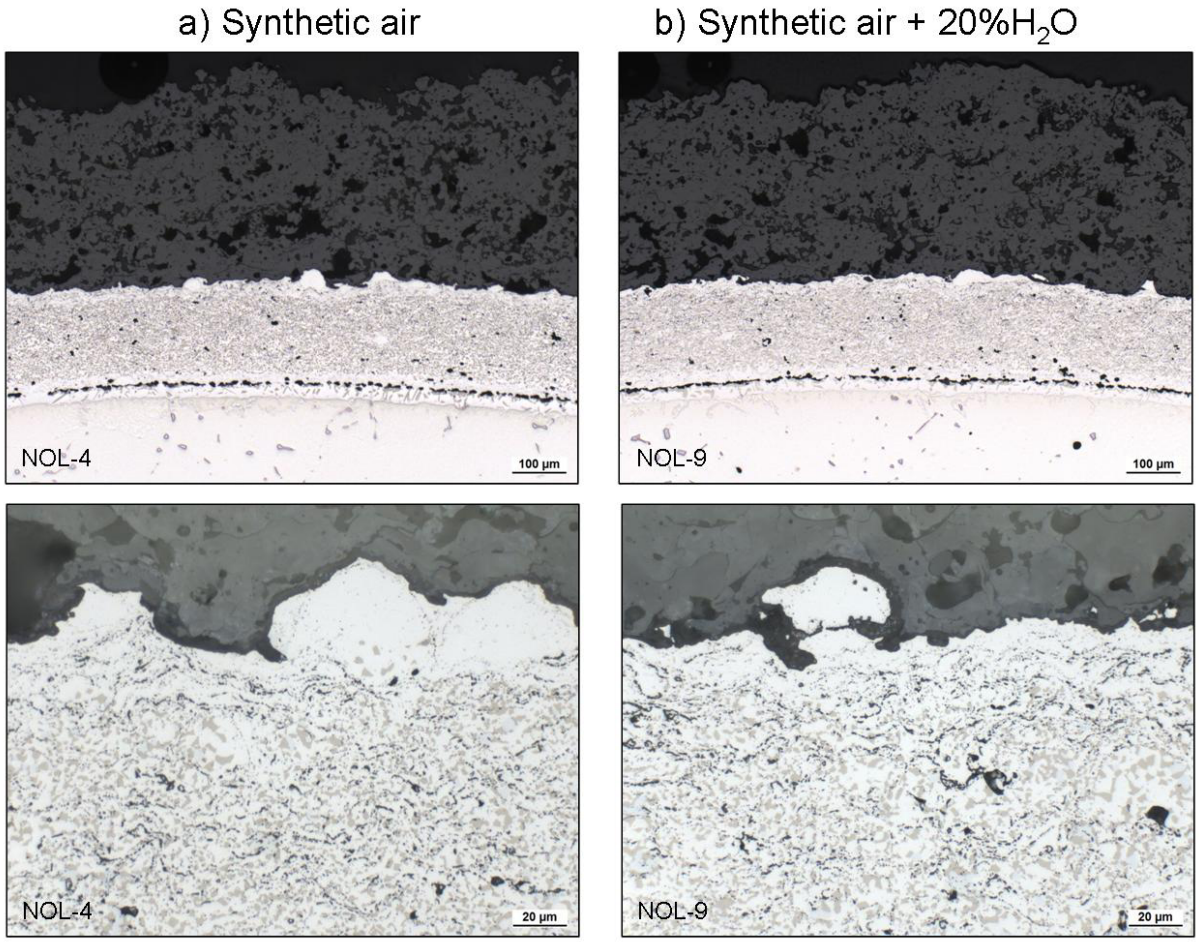

Figure 9: Metallographic cross-sections of the TBC-system NOL: HVOF SC-2231 (FS) + APS-TBC (FS) after 100 h exposure at 1050°C in: a) Synthetic air, b) Synthetic air + 20%H_2O

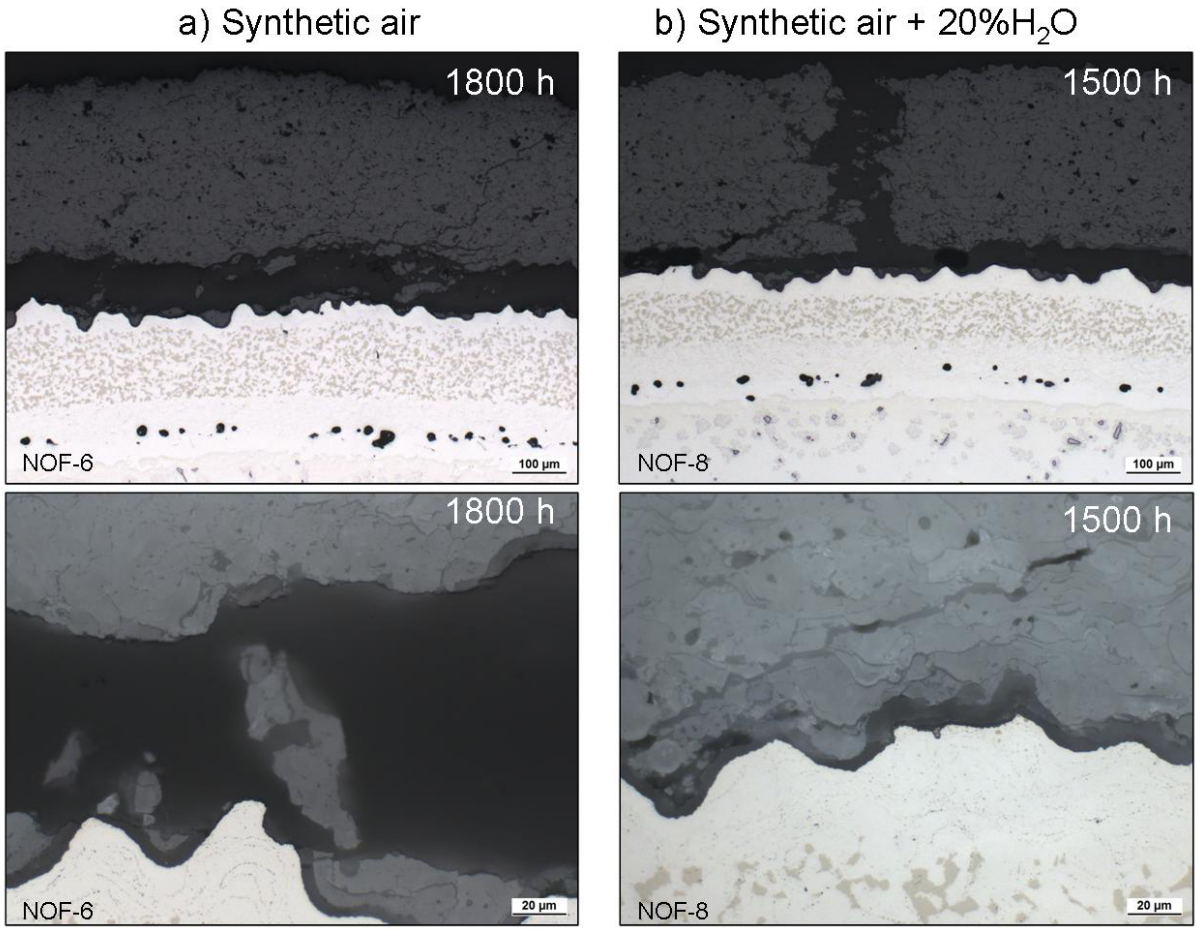

Figure 10: Optical metallographic cross-sections of the TBC system NOF: VPS SC-2464 (FZJ) + APS-TBC (FZJ) after oxidation till TBC failure in: a) Synthetic air, b) Synthetic air + 20%H_2O

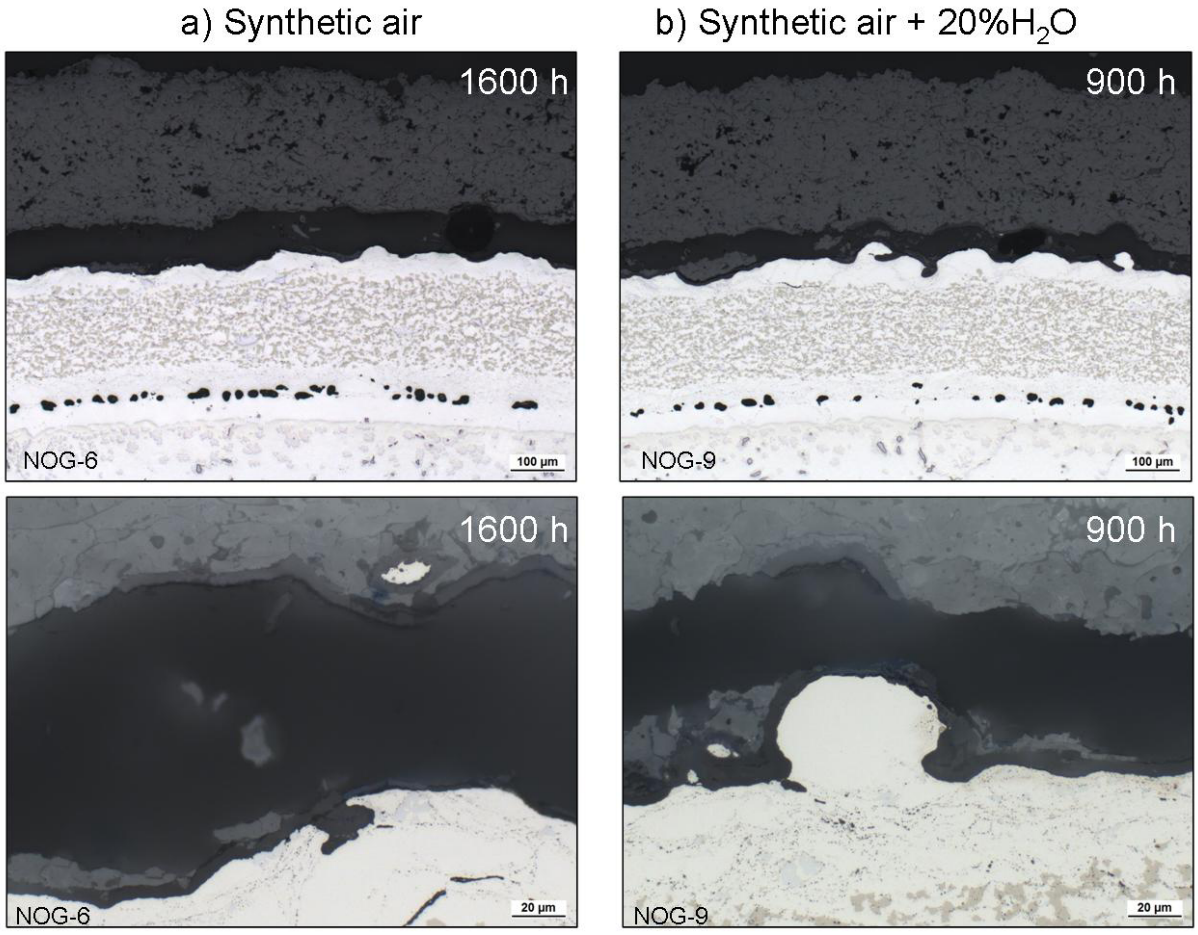

Figure 11: Optical metallographic cross-sections of the TBC system NOG: HVOF SC-2464 (FS) + APS-TBC (FZJ) after oxidation till TBC failure in: a) synthetic air, b) synthetic air + 20%H_2O

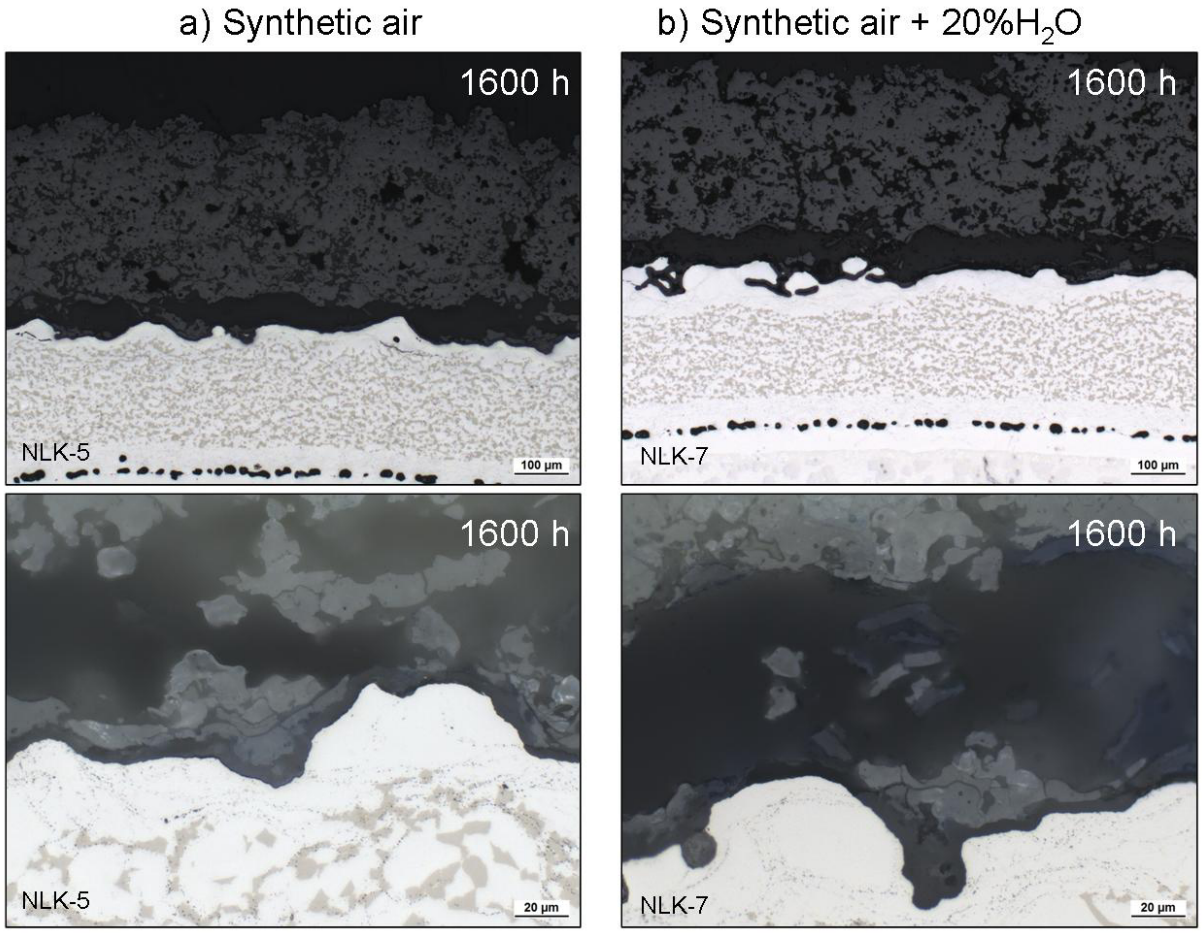

Figure 12: Optical metallographic cross-sections of the TBC system NLK: HVOF SC-2464 (FS) + APS-TBC (FS) after oxidation till TBC failure in: a) synthetic air, b) synthetic air + 20%H_2O

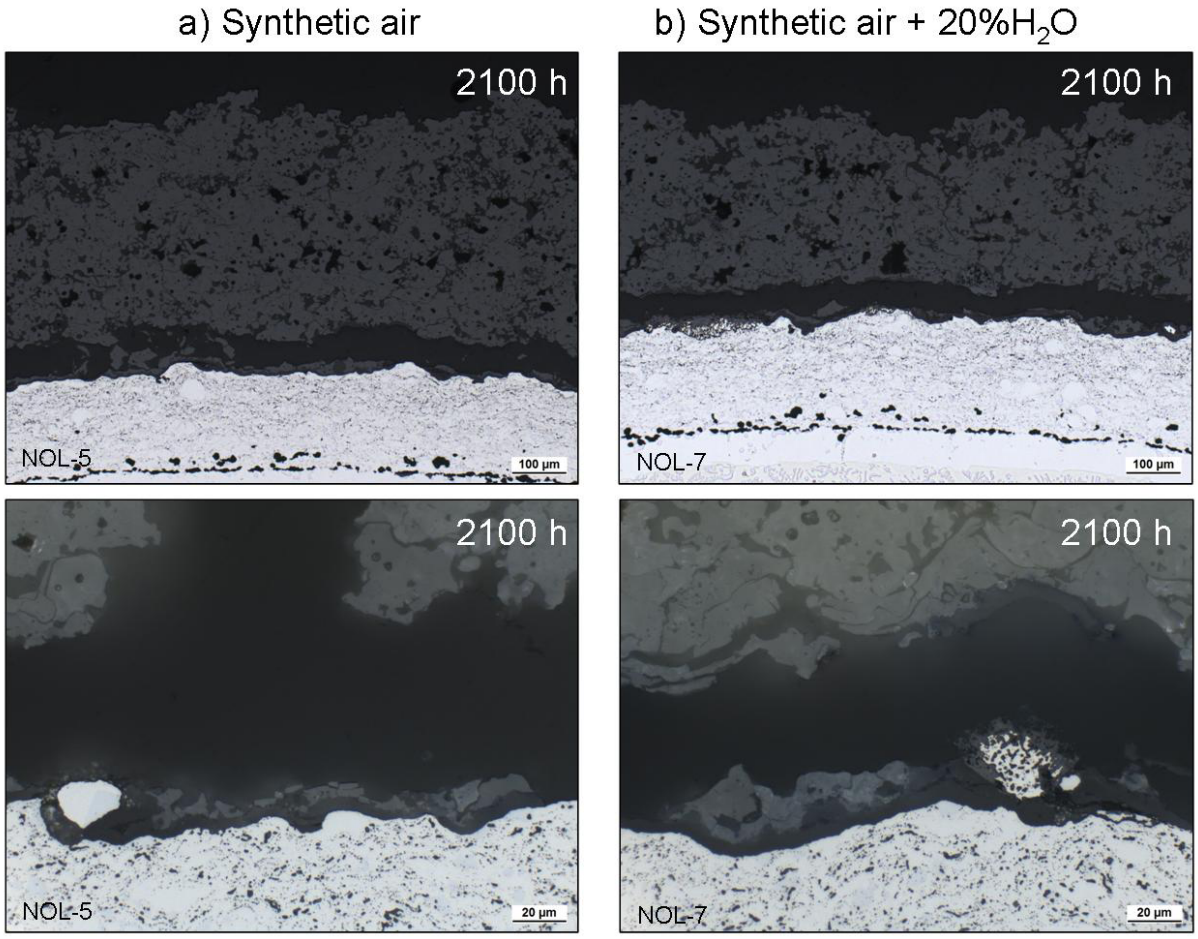

Figure 13: Optical metallographic cross-sections of the TBC system NOL: HVOF SC-2231 (FS) + APS-TBC (FS) after oxidation till TBC failure in: a) Synthetic air, b) Synthetic air + 20%H_2O

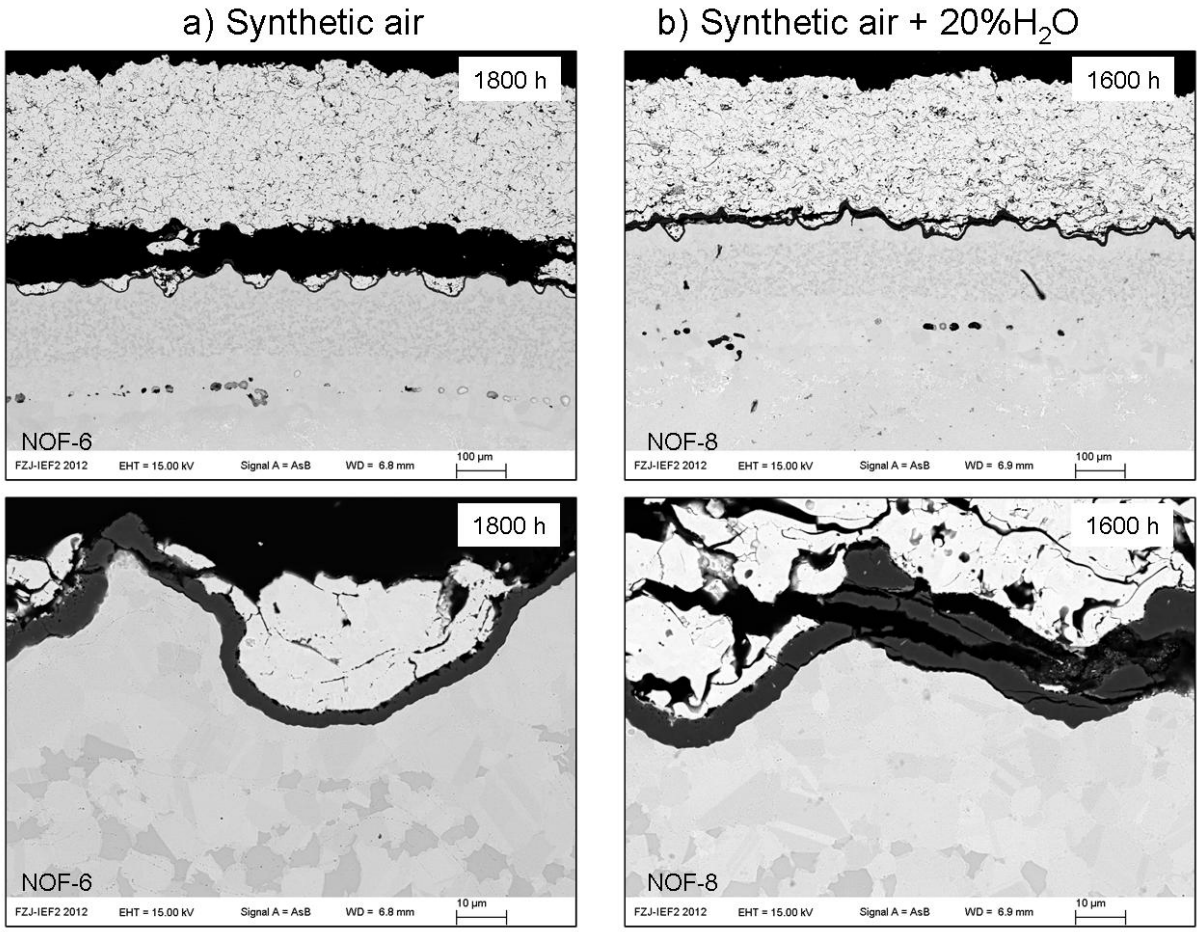

Figure 14: SEM cross-sections of the TBC system: VPS SC-2464 (FZJ) + APS-TBC (FZJ) after oxidation till TBC failure in: a) Synthetic air, b) Synthetic air + 20%H_2O

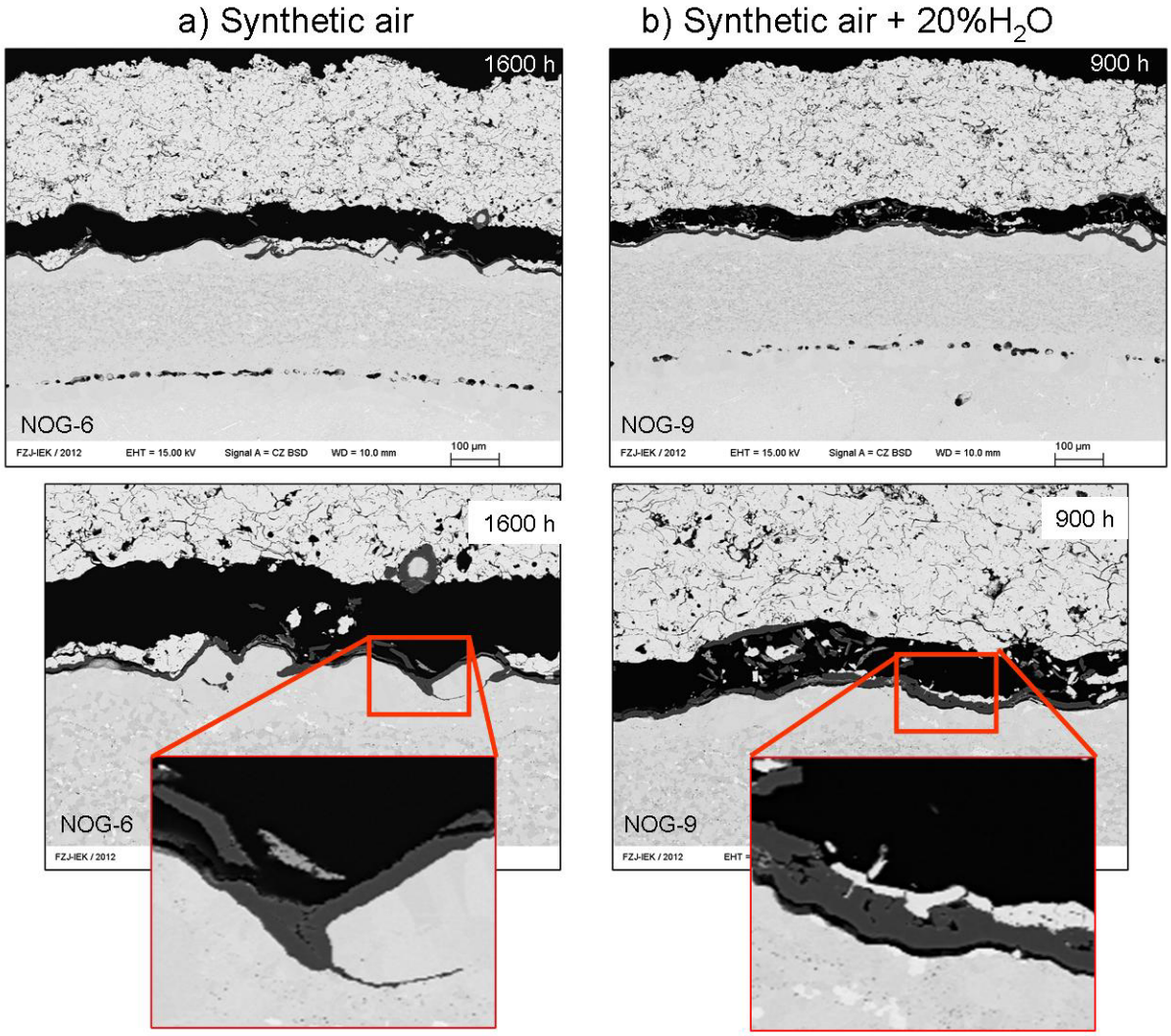

Figure 15: SEM cross-sections of the TBC system: HVOF SC-2464 (FS) + APS-TBC (FZJ) after oxidation till TBC failure in: a) Synthetic air, b) Synthetic air + 20%H_2O

Burner Rig Testing with and without corrosive agent

Experimental

Coating sytems

Four variants of state-of-the-art TBC system with Yttria stabilized zirconia ceramic top coat have been manufactured and submitted to burner rig testing. Three systems with SiCoat 2464 bond coat chemistry on Rene 80 substrates representative for first row blade materials have been produced aiming to examine the influence of manufacturing technology and facilities. A fourth system with SiCoat 2231 bond coat chemistry on Hastelloy X substrates have been considered as representation of wall component materials.

Based on coating manufacturer, coatings deposited by Flame Spray (FS) used high velocity oxygen fuel (HVOF) for the bond coats and atmospheric plasma spraying (APS) for the thermal barrier coatings (TBC). The samples manufactured by Forschungszentrum Jülich (FZJ) used vacuum plasma spraying (VPS) / low pressure plasma spraying (LPPS) to deposit bond coats and APS for the ceramic top coats.

Table 2: Summary table of properties of as-sprayed coatings / samples as reported by manufacturers

Substrate material	Coating manufacturer (BC/TBC)	BC			TBC	
		BC Material	Ra, um	Thickness, um	Thickness, um	Porosity, %
Rene 80	FS/FZJ	SC2464	10.3*	220	340	15
Rene 80	FS/FS	SC2464	10.2	210	350	16
Rene 80	FZJ/FZJ	SC2464	13.9	250	290	(15)
Hastelloy X	FS/FS	SC2231	9,4	230	350	n.a.

Burner rig setup and test conditions

The burner was operated with a natural gas/oxygen mixture. For each cycle during the heating phase the burner flame was positioned on the sample surface of the sample, while the back side was simultaneously cooled with compressed air, establishing a temperature gradient through the sample. During the cooling phase, the burner was moved to the side away from the sample as the sample surface was subsequently cooled with compressed air. Thermal cycles consist of a 5 min heating and a 2 min cooling periods. The surface temperature during testing was measured by an infrared pyrometer with a spot diameter of about 8 mm. The emissivity of the coating was assumed to be one for the pyrometer measurements, which leads to underestimated actual temperatures. To measure the substrate temperature, a NiCr/Ni thermocouple was inserted in a hole radially drilled into the center of the substrate. Target temperatures during heating have been 1250 °C and 1050 °C for surface and substrate, respectively.

The corrosion agents were solutions prepared from colloidal silica and nitrates of calcium, magnesium, aluminum, sodium, potassium, and iron. During thermal gradient cyclic test, the corrosion agent (CMAS or CMAF, refer to Table 3: Composition of corrosive agent based on mol% of cation species) was directly injected and atomized into the burner flame through the central axis of the burner nozzle. This can be manifested by the orange discoloration of the flame from the center of the burner nozzle, Figure 16. The feeding rate of the solution was of 1.2 g/min. Therefore for a 5 min, heating period in which the burner is positioned in front of the sample, an amount of 6 mg of the solution was applied on the sample per test cycle. Thermal cycling tests were stopped when significant degradation of the coating was found, i.e. delamination of the coating at the bondcoat/TBC interface extending over more than half of the sample surface area or exfoliation of small coating lamellae about 5 mm in diameter. After testing, metallographic and phase evolution investigations were conducted to determine the mechanism of failure of the coatings.

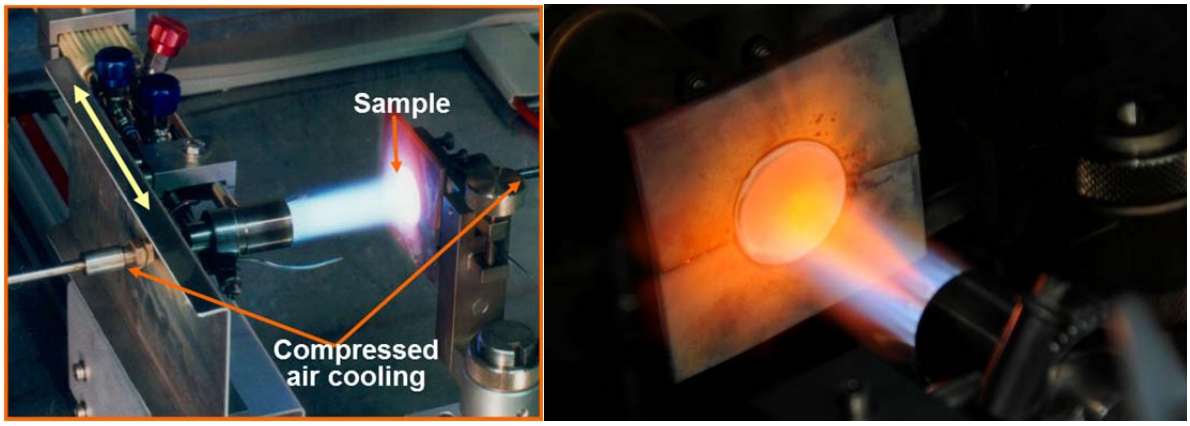

Figure 16: Experimental set-up of the CMAS corrosion test in a burner rig at FZJ. The red flame indicates the infusion of a corrosion agent into the gas stream

Table 3: Composition of corrosive agent based on mol% of cation species

	Ca	Mg	Al	Si	Fe	Na	K
"CMAS"	38	5	4	50	1	1	1
"CMAF"	26	11	9	13	43	0	0

Results

Burner rig test without corrosion agent

To evaluate potential degradation due to thermo-mechanical loads only without the influence of attack from corrosive agents each one sample of the TBC systems under study have been tested without injection of any corrosive media. The duration of this test has been limited to the longest lifetime to failure observed with corrosive media applied, which has been roughly 400 cycles of 5 minutes heating and 2 minutes cooling.

During the test duration of 400 cycles none of the specimen showed macroscopic damage. Figure 17 to Figure 20 show, that the surfaces of the thermally cycled samples without any corrosion agent remain intact.

However, slight changes in color were observed. Sample with Rene 80 substrate coated with SC 2464 HVOF bond coat by FS and YSZ APS TBC by FZ before testing was pale yellow (Figure 17a) before testing and turned to a lighter shade of gray (Figure 17b) after testing. This appearance of the TBC is similar for all samples coated by FZJ as in Figure 19.

Sample with Rene 80 substrate coated with SC 2464 HVOF bond coat by FS and YSZ APS TBC by FS before testing was pale yellow (Figure 18a) before testing and turned into a darker shade of yellow (Figure 18b) after testing. This is similarly observed for all samples with TBC deposited by FS, regardless of the substrate material as in Figure 20 where the substrate is Hastelloy X.

All the tested samples exhibit similar crystallographic patterns after 400 cycles at ~1250°C/1050°C surface and substrate temperatures giving no indication for unusual phase changes or degradation.

The cross-section microstructures of the thermally cycled samples without corrosive agent are shown in Figure 22 to Figure 25. Metallographic investigations conducted, show that 400 cycles at ~1250°C/1050°C did not cause any significant growth of the TGO layer. The measured average values only range around 1-2 microns. However, the height of the depletion zone (measured from the TGO layer to the upper layer of the β-zone) of the bondcoats differ. The sample with Rene 80 substrate which bondcoat and TBC were sprayed by FZ had the most depleted zone (~15 μm) as shown in Figure 22, whereas the samples which bondcoat (regardless of the substrate material) were sprayed by FS using HVOF have minimally depleted zones with only ~5-8 μm. The thicknesses of the TGO layer of these samples fall at the lower range.

At the bondcoat of the sample with Rene 80 substrates coated with SC 2464 HVOF bond coat by FS and YSZ APS TBC by FZJ, rounded areas indicated by arrows in Figure 22 can be observed. These areas have depleted β-phase and occur randomly through the whole bond coat. No elemental analysis was conducted yet on this area. However it is believed to be due to the presence of some Cr-rich impurity deposited during HVOF that poisons the formation of β-phase in these areas.

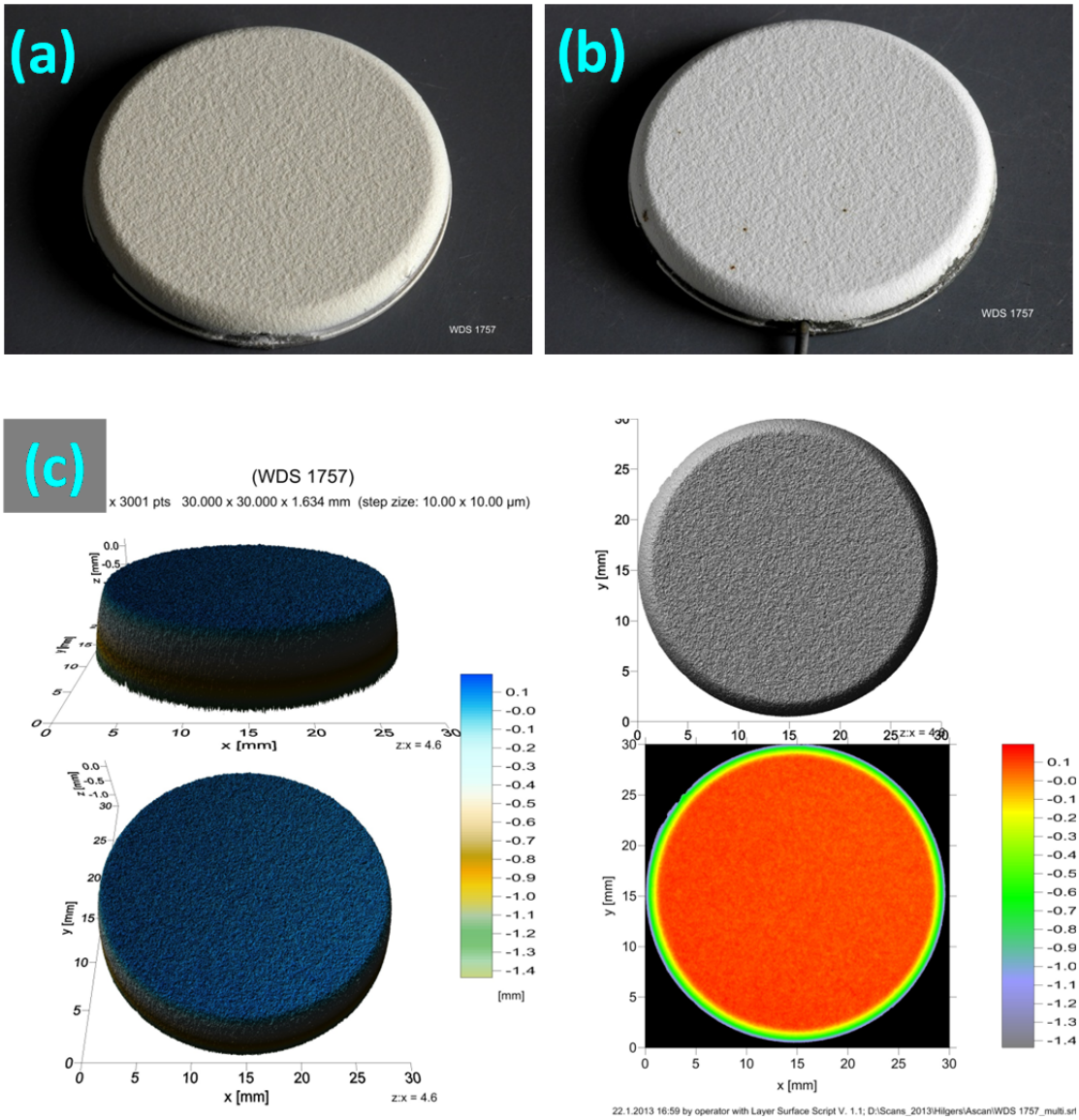

Figure 17: Photograph of sample with Rene 80 substrate coated with SC 2464 HVOF bond coat (FS) and YSZ APS TBC (FZ) (a) before and (b) after testing without CMAS at 1250°C/1050 surface/substrate temperature. (c) is surface profile after testing

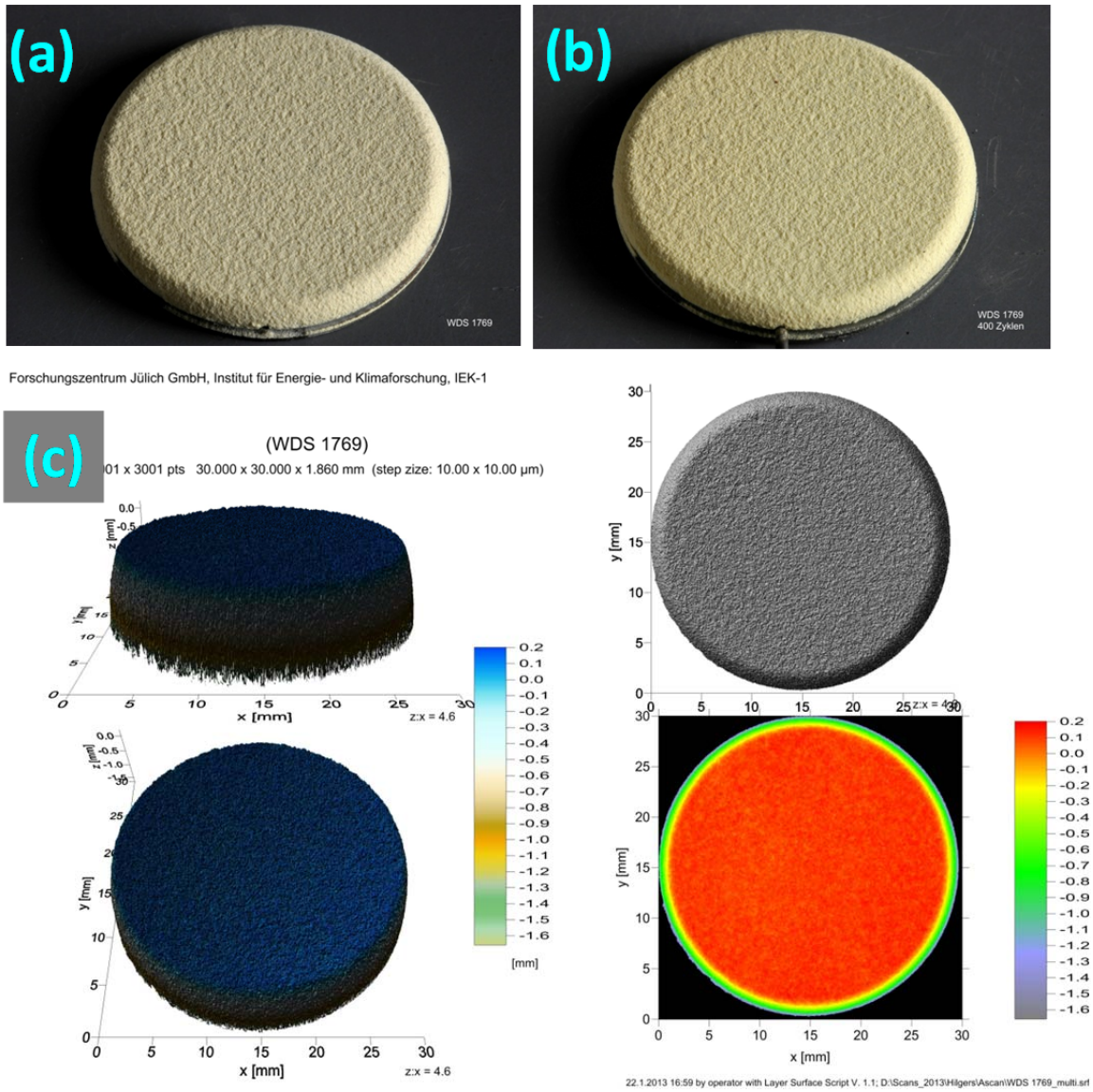

Figure 18: Photograph of sample with Rene 80 substrates coated with SC 2464 HVOF bond coat (FS) and YSZ APS TBC (FS) (a) before and (b) after testing without CMAS at 1250°C/1050 surface/substrate temperature. (c) is surface profile after testing

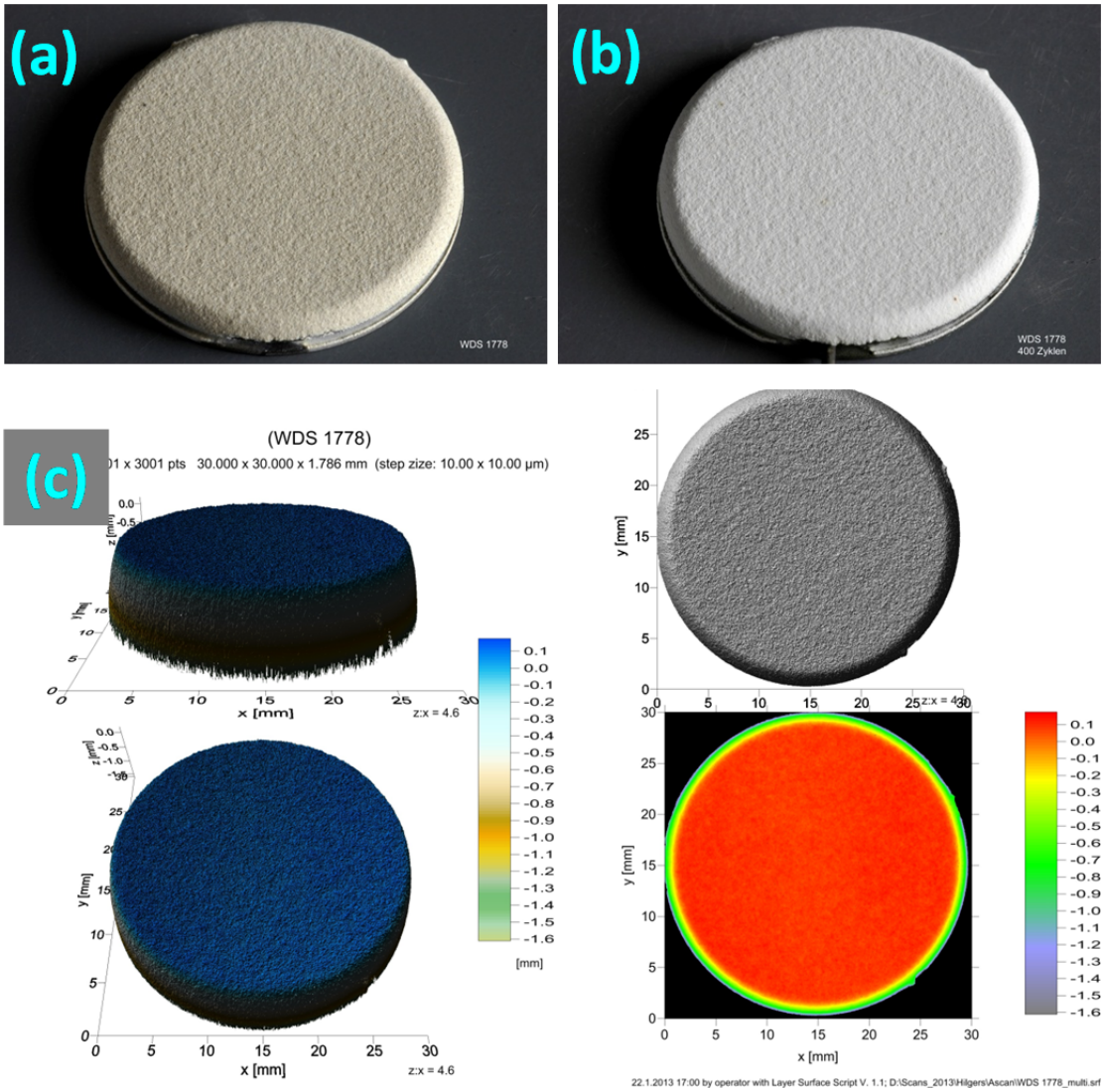

Figure 19: Photograph of sample with Rene 80 substrates coated with SC 2464 VPS bond coat (FZJ) and YSZ APS TBC (FZJ) (a) before and (b) after testing without CMAS at 1250°C/1050 surface/substrate temperature. (c) is surface profile after testing

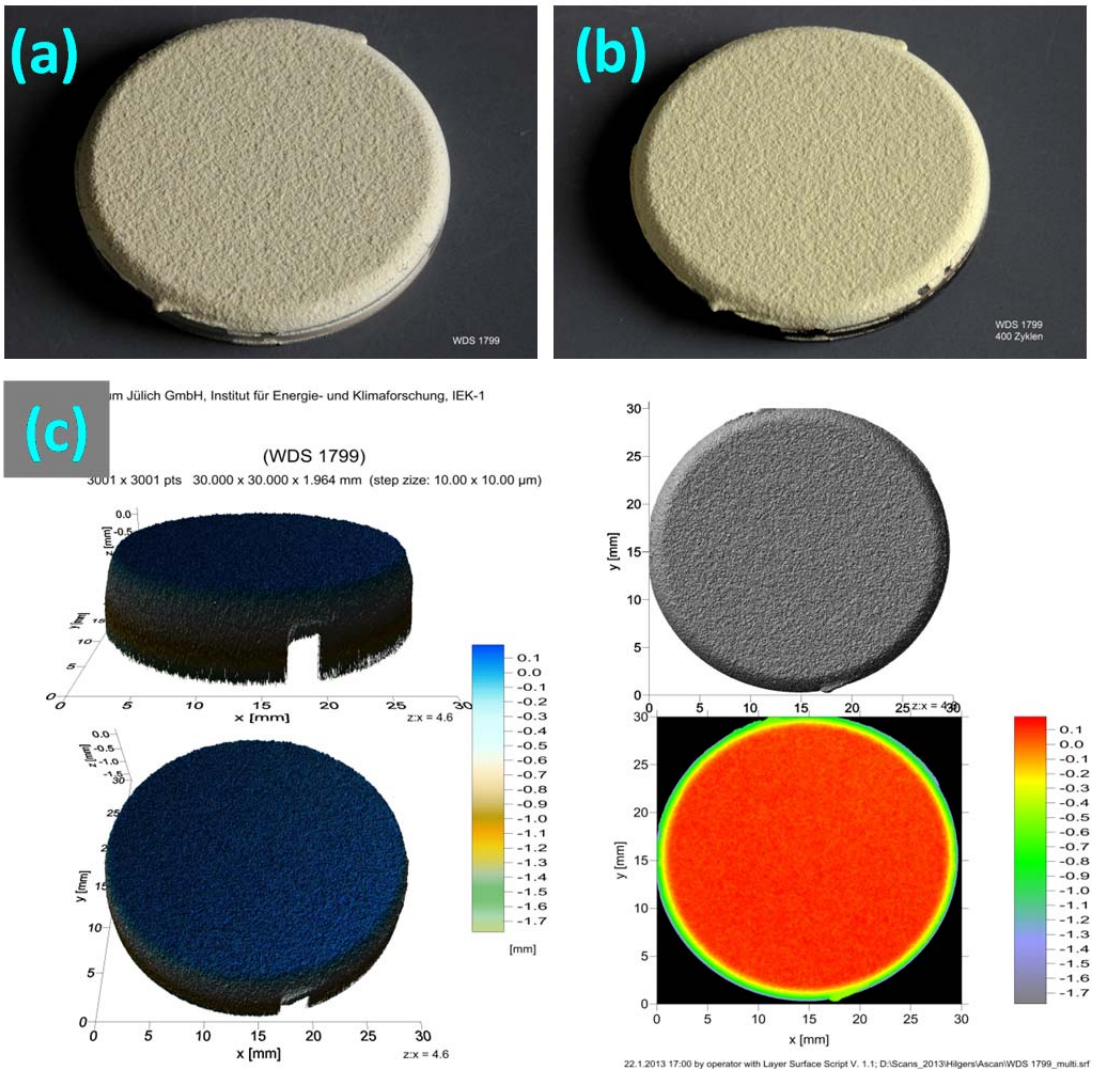

Figure 20: Photograph of sample with Hastelloy X substrates coated with SC 2464 HVOF bond coat (FS) and YSZ APS TBC (FS) (a) before and (b) after testing without CMAS at 1250°C/1050 surface/substrate temperature. (c) surface profile after testing

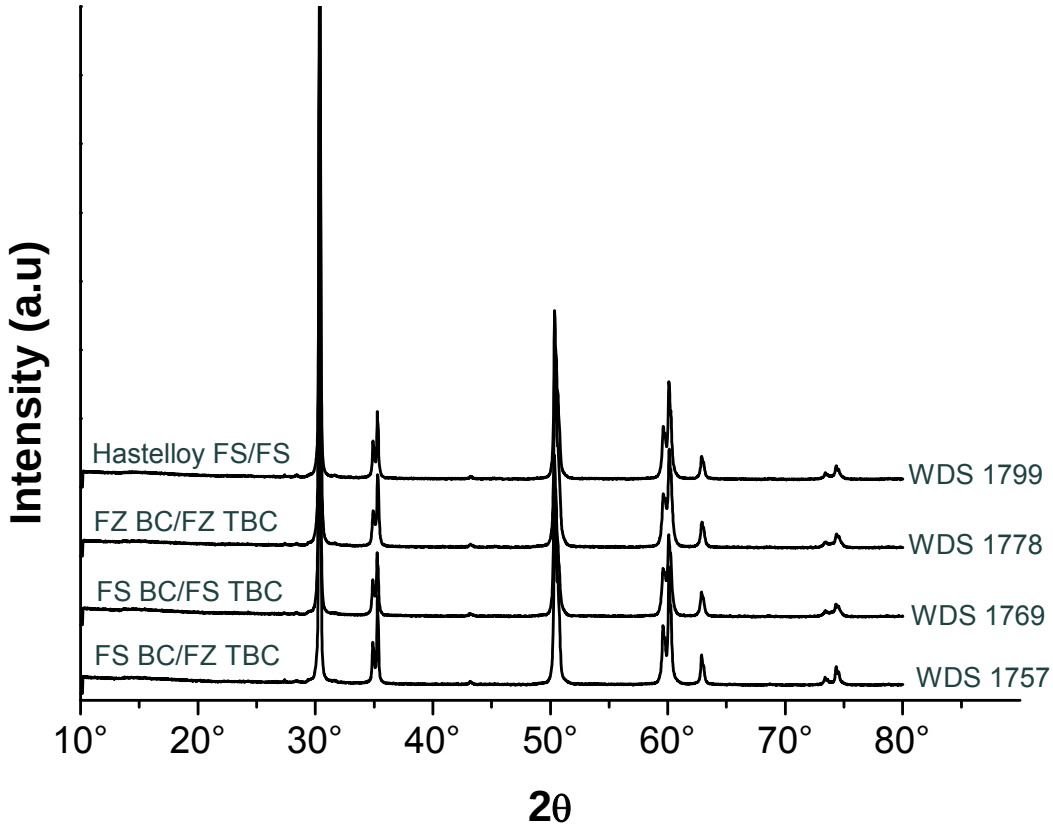

Figure 21: XRD profile of samples cycled without corrosion agent at 1250°C/1050°C surface/substrate temperature

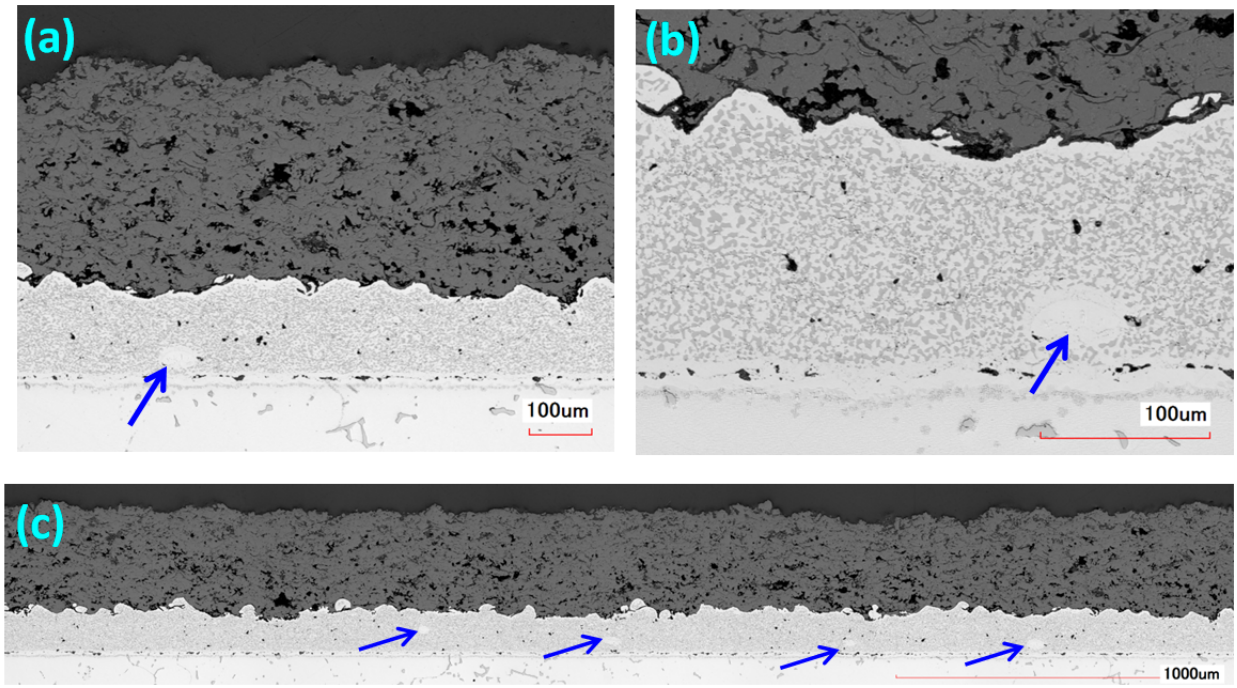

Figure 22: Cross-section images of sample with Rene 80 substrates coated with SC 2464 HVOF bond coat (FS) and YSZ APS TBC (FZJ) after thermal cycling without CMAS at 1250°C/1050 surface/substrate temperature

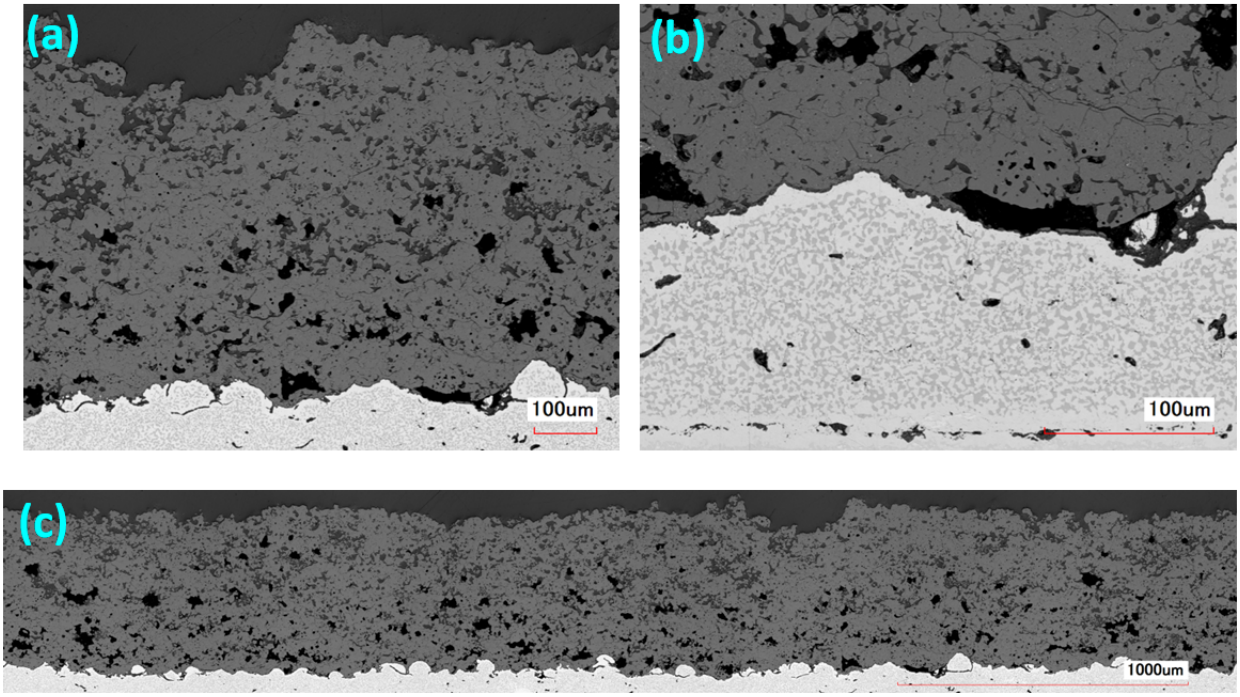

Figure 23: Cross-section images of sample with Rene 80 substrates coated with SC 2464 HVOF bond coat (FS) and YSZ APS TBC (FS) after thermal cycling without CMAS at 1250°C/1050 surface/substrate temperature

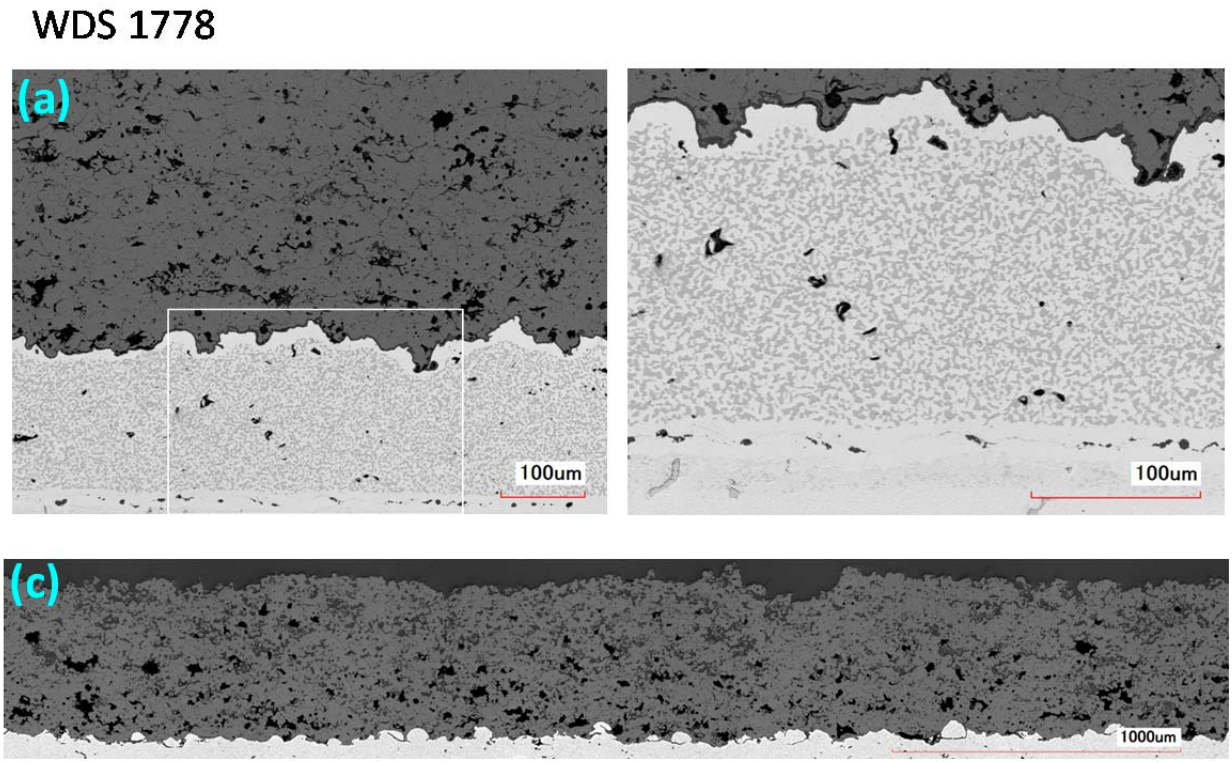

Figure 24: Cross-section images of sample with Rene 80 substrates coated with SC 2464 VPS bond coat (FZJ) and YSZ APS TBC (FZJ) after thermal cycling without CMAS at 1250°C/1050 surface/substrate temperature

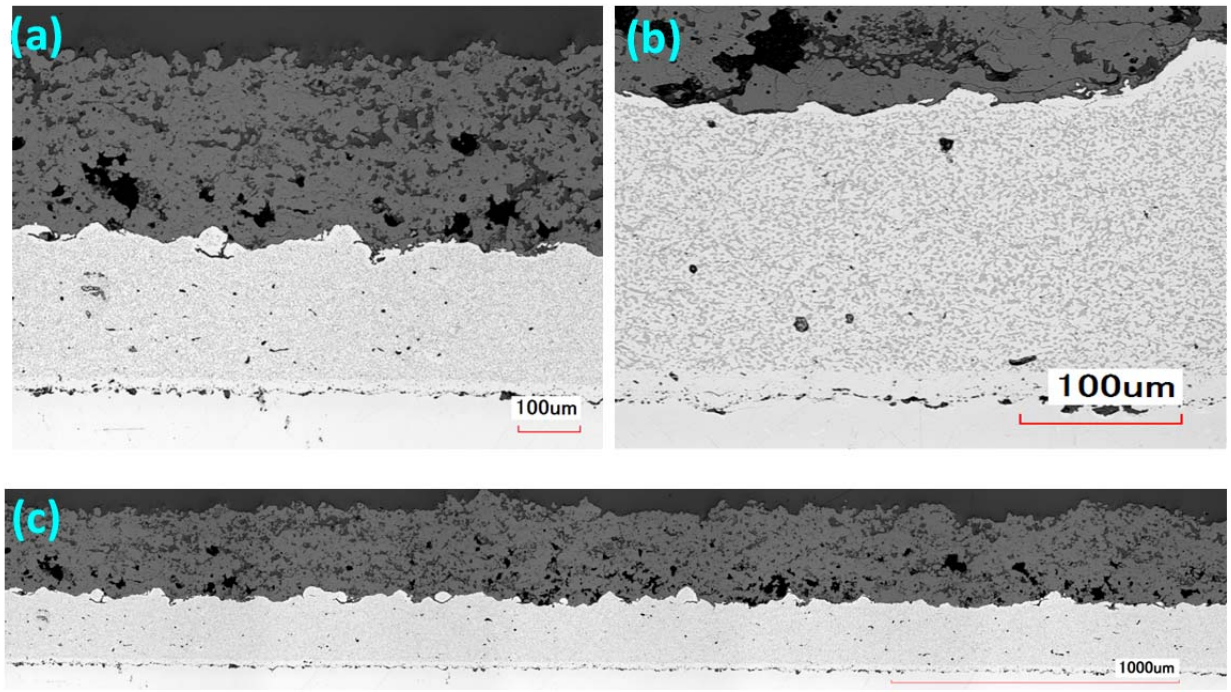

Figure 25: Cross-section images of sample with Hastelloy S substrates coated with SC 2464 HVOF bond coat (FS) and YSZ APS TBC (FS) after thermal cycling without CMAS at 1250°C/1050 surface/substrate temperature

Burner rig test with CMAS agent

Figure 26: Number of cycles until failure for the samples exposed to CMAS corrosion at 1250°C/1050°C surface/substrate temperature (target values) summarizes the number of cycles until failure for the samples exposed to CMAS corrosion at 1250°C/1050°C surface/substrate temperature (target values). Although the chemistry of topcoat is nominally equal for all samples the cycling performance under CMAS attack is remarkable different. Nearly one order of magnitude in cycling lifetime is observed for TBC systems manufactured by Flame Spray on substrate material Rene 80 or Hastelloy X, respectively.

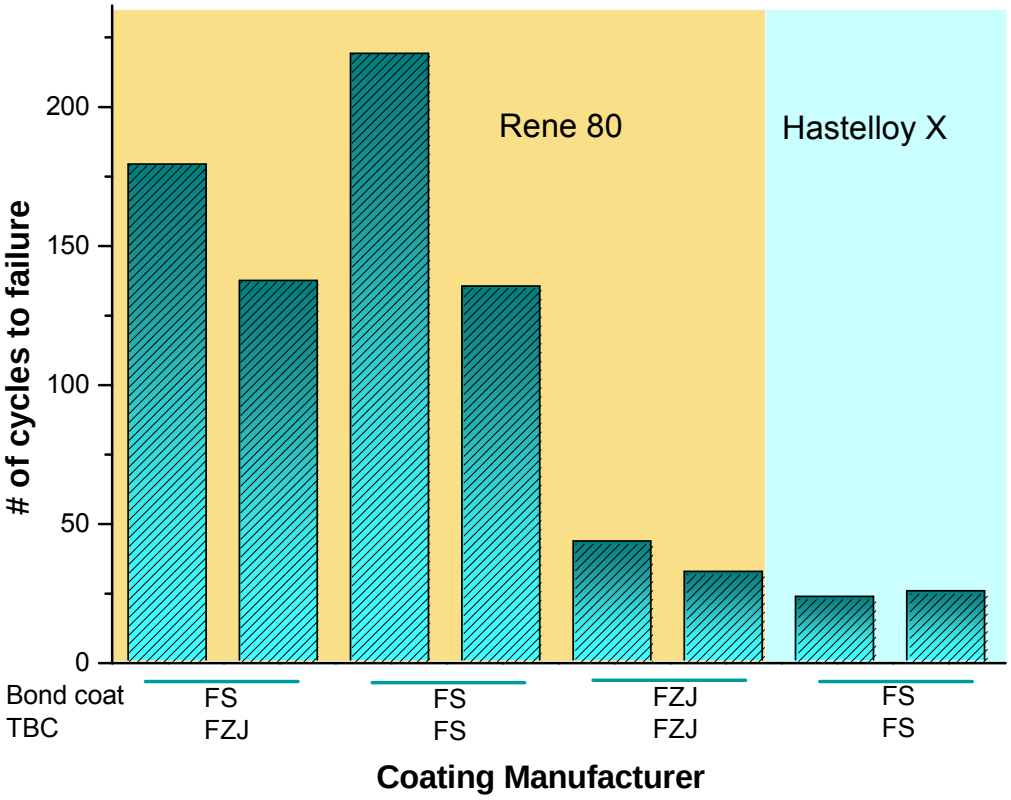

Figure 26: Number of cycles until failure for the samples exposed to CMAS corrosion at 1250°C/1050°C surface/substrate temperature (target values)

Figure 27 shows photographs of samples after testing. For the right sample in row (a) there was a lifting of about 800 µm from the surface of the TBC before spallation took place. The sample on the left in Figure 27(c), has a lifting of about 600 micrometers from the surface. The failure mode for nearly all of the samples with Rene 80 substrate seems to start with lifting of about 10mm diameter surface at the center of the sample before spalling-off. Delamination cracks are found to be near to the bondcoat interface (deep) within the ceramic. The spallen TBC left in Figure 27(b) was reattached for photography just to show the failure mode of the coating. There was formation of glassy white deposits where the coating spallation occurred.

Tested samples with Hastelloy X substrates seem to have a stepwise chip by chip (shallow) degradation at the surface (Figure 27(d)). These samples have relatively low substrate temperatures. The target substrate temperature of 1050°C was quite difficult to establish during testing.

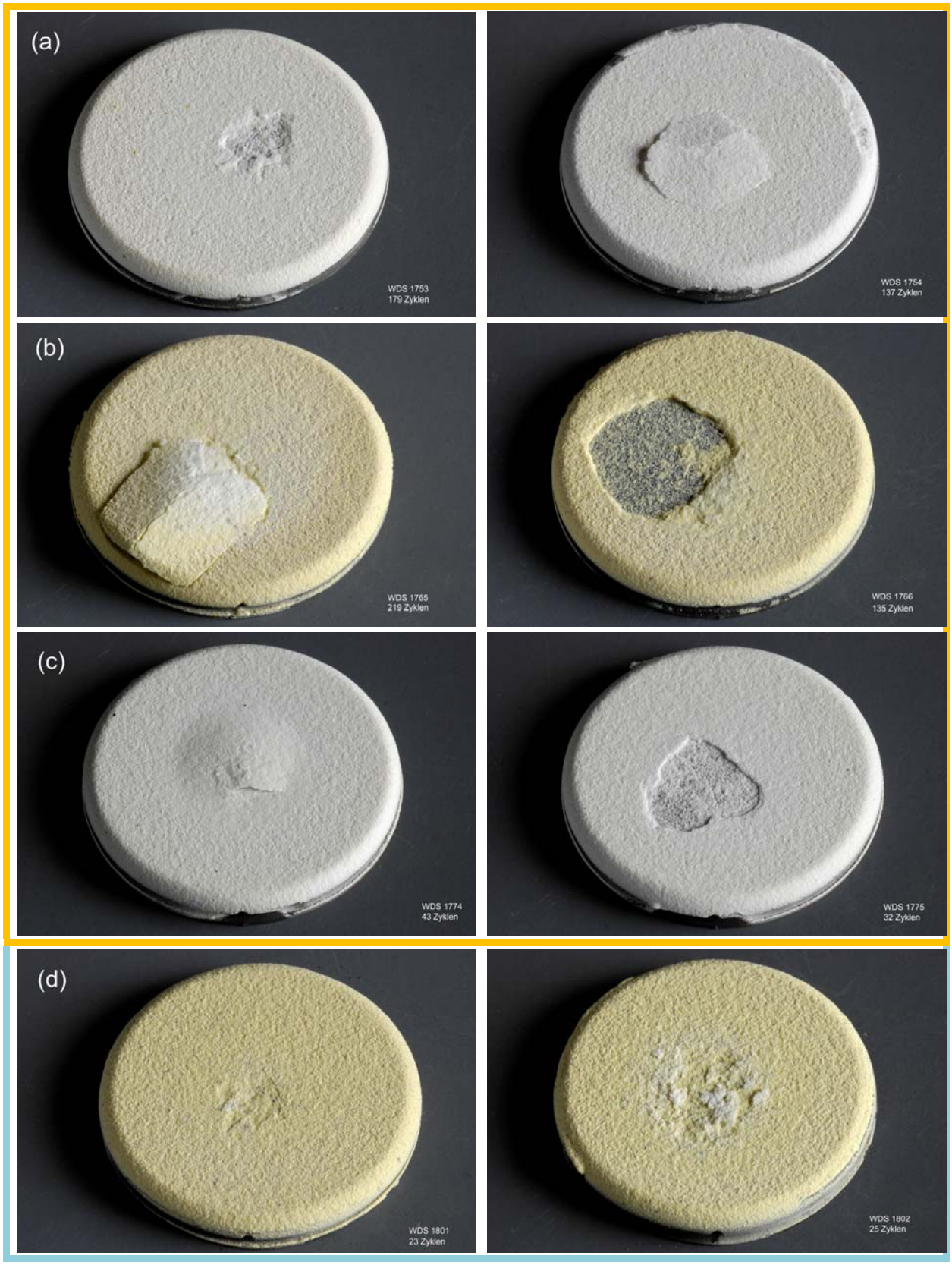

Figure 27: Photograph of samples after testing with CMAS at 1250°C/1050 surface/substrate temperature (target value): Rene 80 with BC SC2464 and TBC YSZ by FS / FZJ (a), FS / FS (b), FZJ / FS (c), Hastelloy X with BC SC2231 and TBC YSZ by FS / FS (d)

The TBC ceramic of coatings manufactured by Forschungszentrum Jülich (Figure 27(a) and (c)) became light gray instead of pale yellow as compared to the as-sprayed sample in Figure 21(a). This has been observed independently on the CMAS deposit as well on those samples cycled without any deposit and is a typically due to re-oxidation of oxygen deficient YSZ.

X-ray diffraction profiles of the samples cycled with CMAS are shown in Figure 28. The patterns are arranged with sample type having the least number of cycles at the bottom and the highest number of cycles at the uppermost. Patterns can be basically evaluated considering (a) tetragonal zirconia originating from the initial not-yet-reacted YSZ, (b) cubic zirconia potentially re-precipitated from the CMAS melt, (c) crystalline phases quenched from the glassy melt as e.g. (pseudo-)wollastonite and anorthite, and (d) mixed oxide phases crystallized from the deposit at elevated temperatures as e.g. akermanite or traces of $ZrSiO_4$.

Individual phases identified by XRD characterization of degraded sample surfaces present a wide range of more specific compositions and large variety of fractions. This is due to the accumulation of reflections from samples owing inhomogeneous degraded surface areas. Nevertheless, review of identified crystalline phases may provide additional indications on the evolution of coating degradation:

The patterns indicate that samples with Hastelloy X (WDS 1801 and WDS 1802) substrates where substrate temperature was difficult to stabilize at 1050°C have the shortest lifetimes. Although majority of the TBC is still composed of tetragonal zirconia, a large amount of pseudowollastonite phase of monoclinic $Ca(SiO_3)_3$ was already detected. Also detected for WDS 1801 are traces of $AlZr_2$ and a metastable monoclinic phase containing Na, Ca, Fe, Al and Si. This sample has more intense peaks of anorthite and pseudowollastonite than WDS 1802.

For samples with Rene 80 substrates which SC 2464 bondcoat and YSZ TBC were deposited by FZJ (WDS 1774 and WDS 1775), the anorthic peaks increased in crystallinity and tetragonal akermanite phases were formed. However, the zirconia peaks exhibit a cubic structure instead. WDS 1774 has similar phases as 1775 however the intensities of akermanite and anorthites are higher. WDS 1775 shows evidence of tetragonal YSZ dissolution as anorthic phases increasingly form.

Considerable high lifetimes were observed for samples with Rene 80 and both coatings sprayed by flame spray (WDS 1753 and WDS 1754). More anorthic and akermanite phases were formed as the number of cycles increased. WDS 1754 has monoclinic baghdadite phase $Ca_3ZrSi_2O_9$ which could not be found in WDS 1753. Traces of cubic $AlCrNi_2$ were probably detected from the exposed TBC-bond coat interface. Metastable monoclinic phase containing Na, Mg and Fe was also detected.

Cycled samples which bond coat was deposited by FS and TBC by FZJ on Rene 80 have the highest lifetimes (WDS 1765 and WDS 1766). On these samples monoclinic $Ca_3ZrSi_2O_9$ are formed. The intensity of these compounds increased with increasing number of cycles. WDS 1765 shows the presence of orthorhombic $Ca_{1.7}Mg_{0.3}SiO_4$ but this phase is very low in WDS 1766. Both contain traces of tetragonal $Ca_2Al((AlSi)O_7)$and $ZrSiO_4$.

Figure 29: SEM Micrographs (a, b) and EDX element mapping (c) of inner area of a sample type substrate Rene 80 with BC SC2464 and TBC YSZ manufactured by FS / FZJ after testing with CMAS at 1250°C/1050 surface/substrate temperature (target value)Figure 29 shows SEM micrographs and an EDX element mapping of a subsurface area after testing of a sample from Rene 80 substrate with SC2464 bondcoat and YSZ TBC which has been manufactured by FS / FZJ. As a showcase it can be clearly observed that the silicious deposit is able to penetrate well below the surface by means of large sized cracks or pores.

The higher the amount of open porosity the more pronounced the infiltration can be expected.

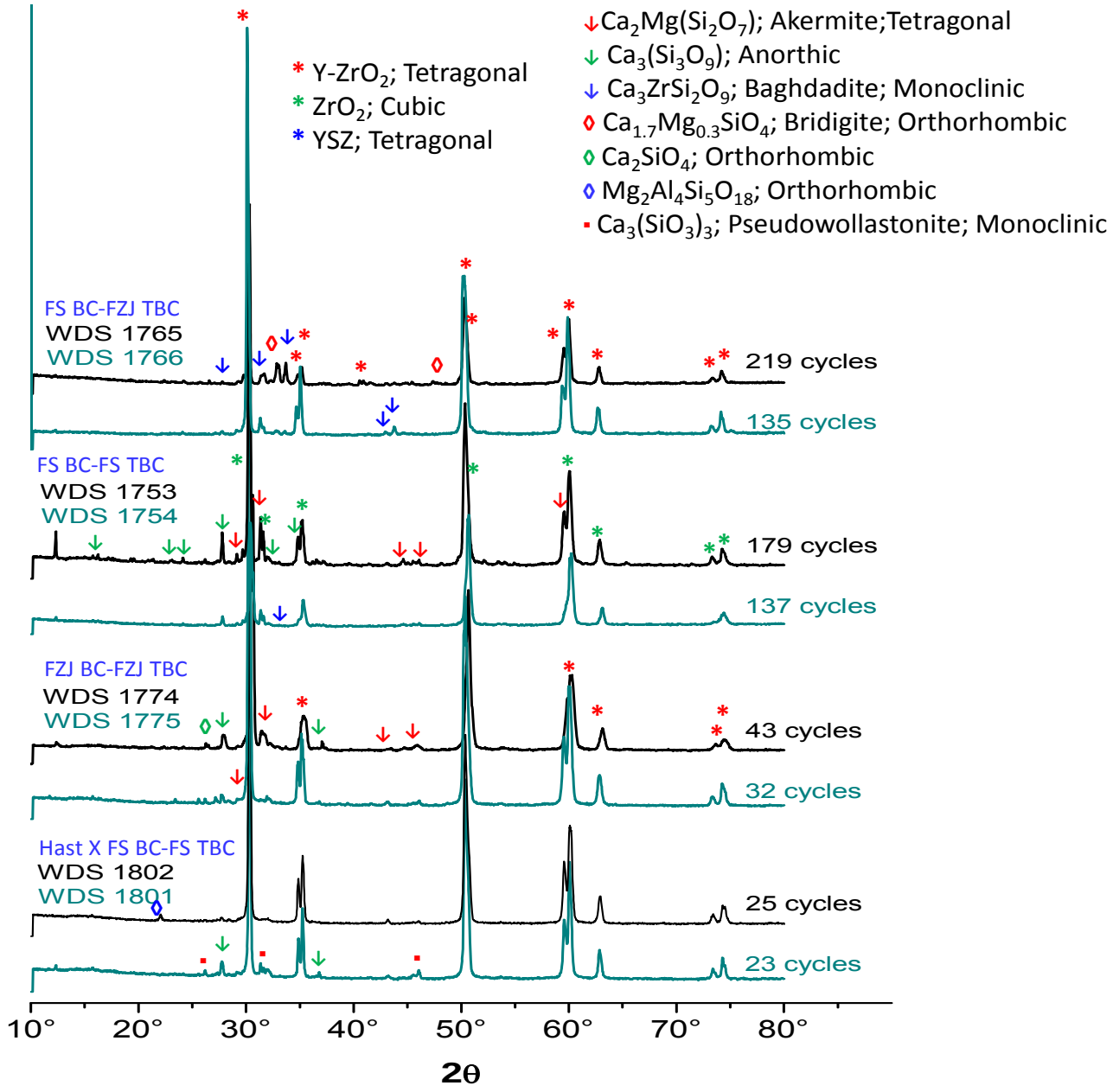

Figure 28: X-ray diffraction profiles of the samples exposed to CMAS corrosion at 1250°C/1050°C surface/substrate temperature until failure of the TBC

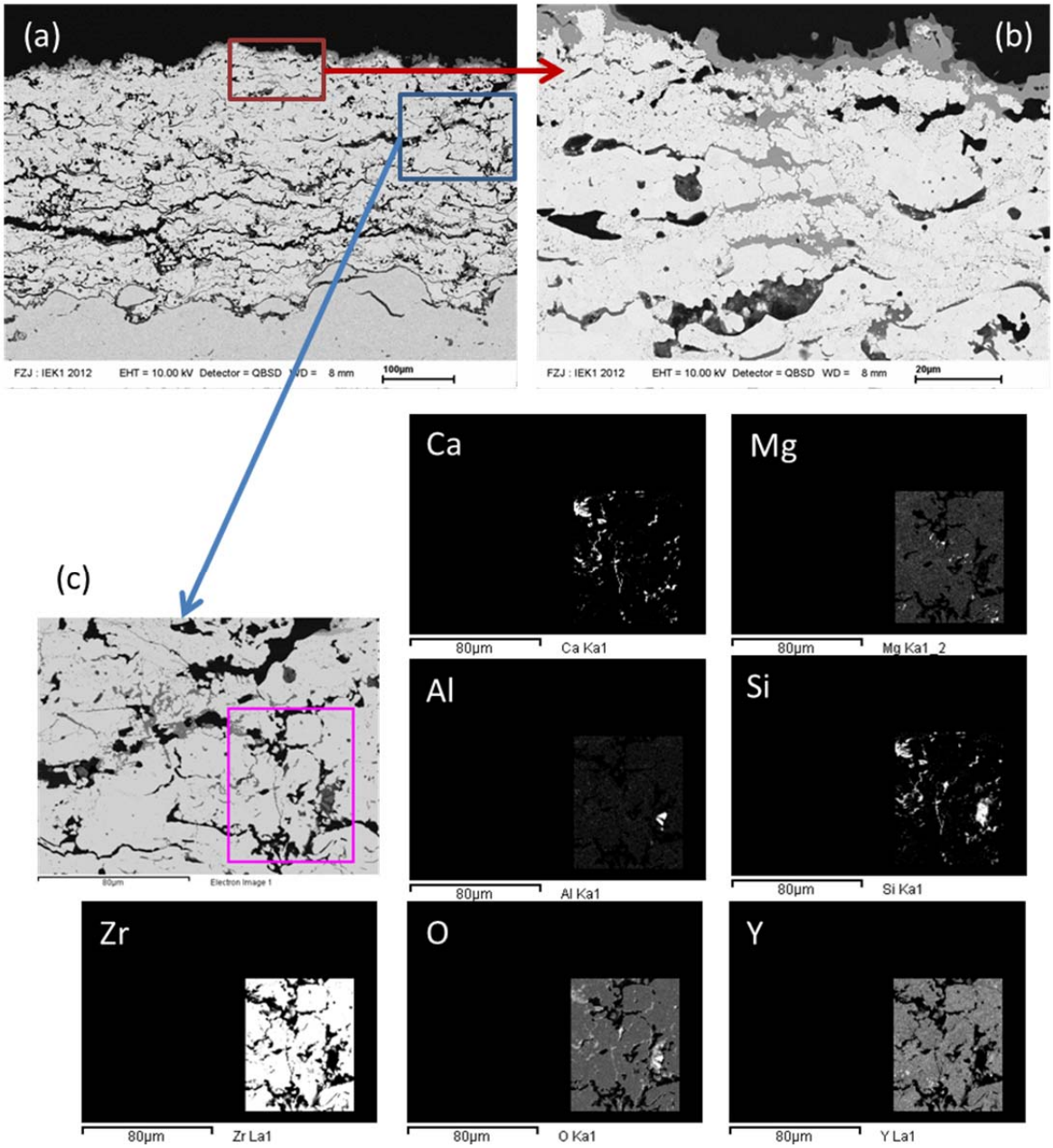

Figure 29: SEM Micrographs (a, b) and EDX element mapping (c) of inner area of a sample type substrate Rene 80 with BC SC2464 and TBC YSZ manufactured by FS / FZJ after testing with CMAS at 1250°C/1050 surface/substrate temperature (target value)

Burner rig test with CMAF agent

Figure 30 summarizes the number of cycles until failure for the samples exposed to CMAF corrosion at 1250°C/1050°C surface/substrate temperature (target values). For all systems an increase in cycling lifetime can be observed. At the same time the scatter of lifetime results among samples of the same type is remarkable increased.

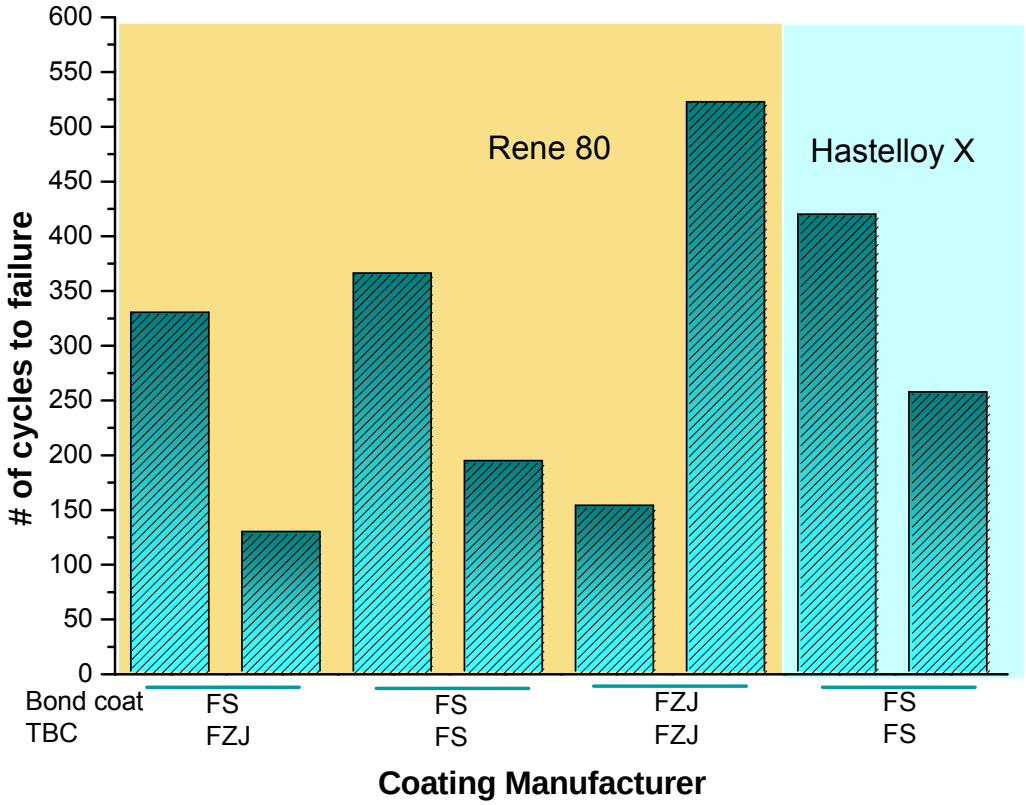

Figure 30: Number of cycles until failure for the samples exposed to CMAF corrosion at 1250°C/1050°C surface/substrate temperature (target values)

Figure 31 shows photographs of samples after testing. Degradation of ceramic topcoats seem to be generally less pronounced compared to attack by CMAS deposit. All sample surfaces are colored reddish what is most probably due to large amounts of Fe^{3+} oxides originating from high iron content in the deposit. Complete spallation is obvious only for one sample (Figure 31(a), left) whereas deep delamination and lifting of the topcoat can only be anticipated in smaller scale for samples on Figure 31(c). For samples with APS coating manufactured by Flame Spray (Figure 31(b) and (c)) the predominant failure mode observed is shipping of surface near ceramic flakes.

Figure 32 shows X-ray diffraction profiles of the samples cycled with CMAF. Patterns can be basically evaluated in a similar manner as in the case of zirconia coatings degraded by CMAS type deposit. Major differences appear to be the lower amount of remaining tetragonal zirconia and high amounts of mixed magnesia iron spinel phase. Individual phases identified by XRD characterization of degraded sample surfaces again present a wide range of more specific compositions and large variety of fractions.

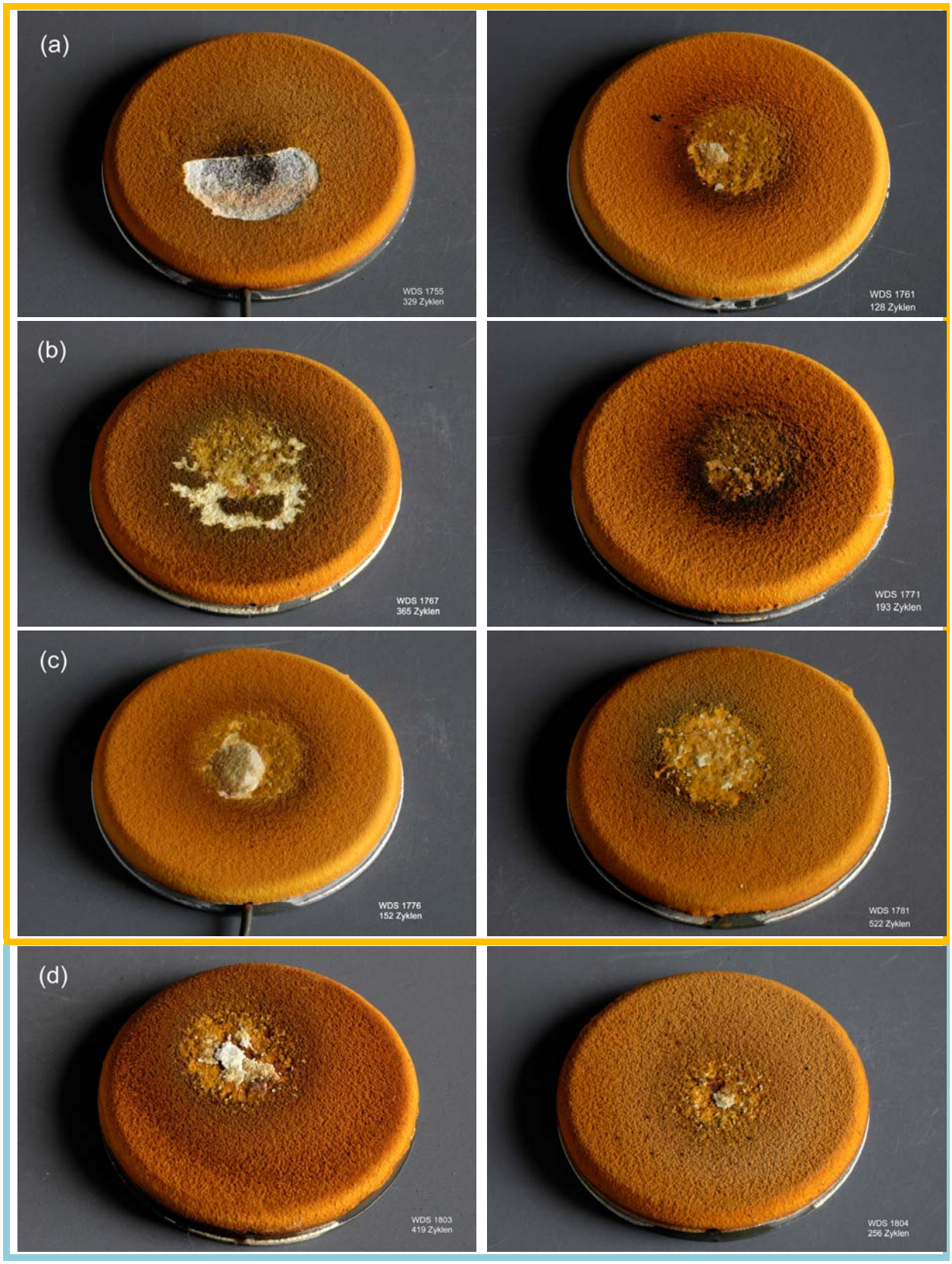

Figure 31: Photograph of samples after testing with CMAF at 1250°C/1050 surface/substrate temperature (target value): Rene 80 with BC SC2464 and TBC YSZ by FS / FZJ (a), FS / FS (b), FZJ / FS (c), Hastelloy X with BC SC2231 and TBC YSZ by FS / FS (d)

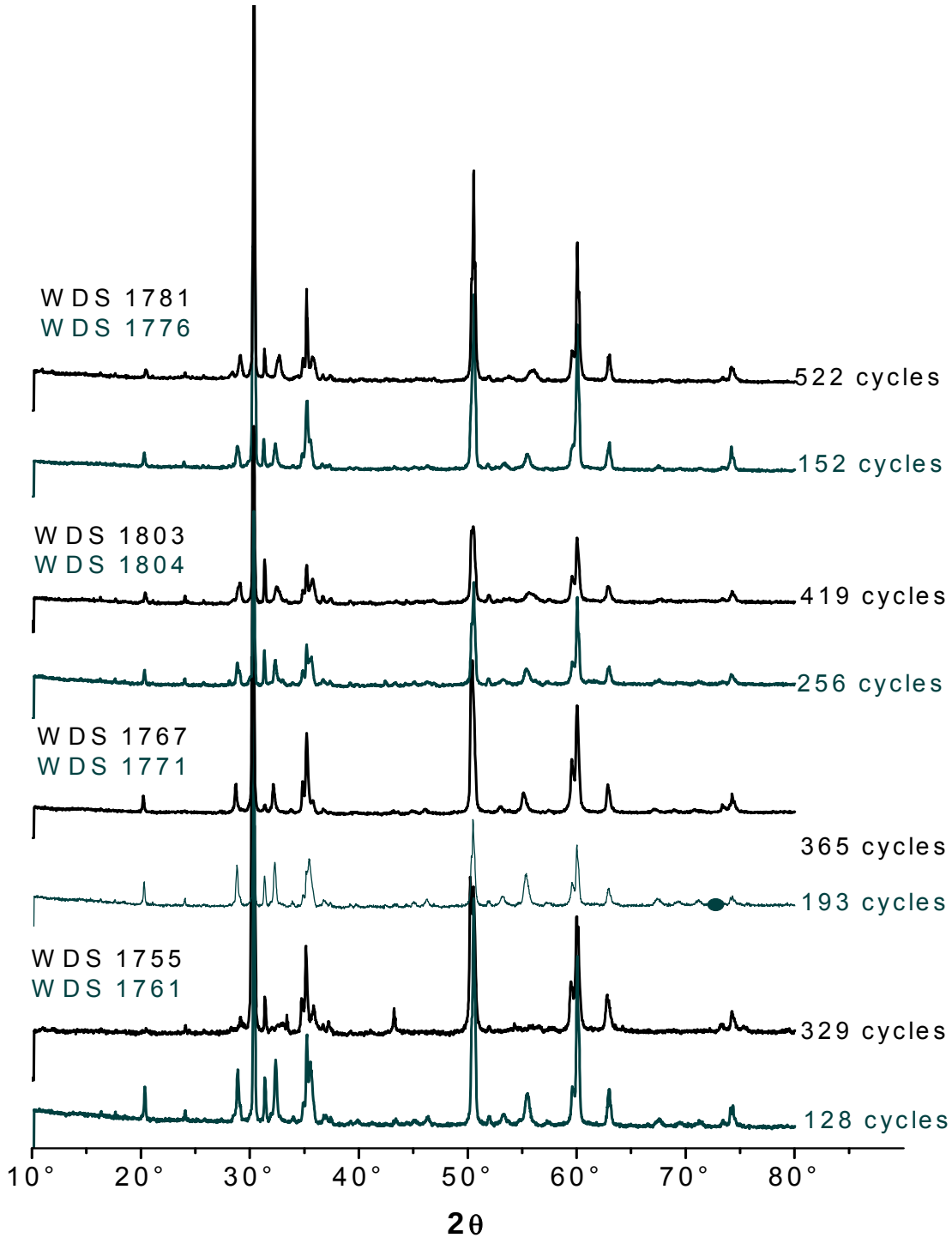

Figure 32: X-ray diffraction profiles of the samples exposed to CMAF corrosion at 1250°C/1050°C surface/substrate temperature until failure of the TBC

Figure 29: SEM Micrographs (a, b) and EDX element mapping (c) of inner area of a sample type substrate Rene 80 with BC SC2464 and TBC YSZ manufactured by FS / FZJ after testing with CMAS at 1250°C/1050 surface/substrate temperature (target value)Figure 33 shows SEM micrographs and an EDX element mapping of a subsurface area after testing of

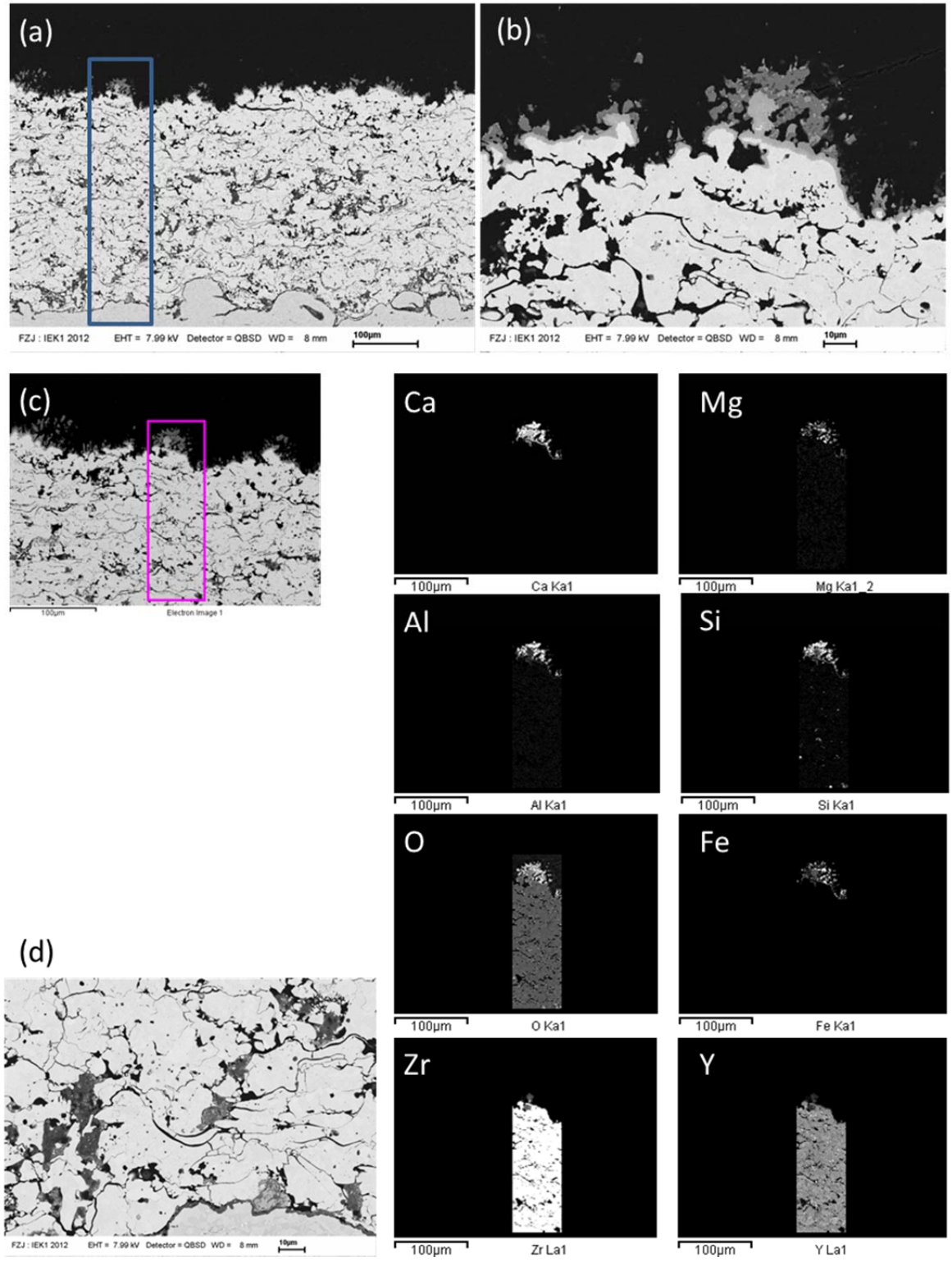

Figure 33: SEM Micrographs (a, b, d) and EDX element mapping (c) of inner area of a sample type substrate Rene 80 with BC SC2464 and TBC YSZ manufactured by FS / FZJ after testing with CMAF at 1250°C/1050 surface/substrate temperature (target value)

a sample from Rene 80 substrate with SC2464 bondcoat and YSZ TBC which has been manufactured by FS / FZJ. As a showcase it can be clearly observed that the silicious deposit is able to penetrate well below the surface by means of large sized cracks or pores. Nevertheless, compared to low iron CMAS deposit the infiltration in the surface near region appears to be less pronounced. High iron content oxides are arrested on top of the coating.

Summary and Outlook

Performance of state-of-the-art YSZ thermal barrier coating systems under simultaneous load from thermal gradient cycling and corrosive CMAS/F attack is summarized in Table 4. Although the chemistry of topcoat is nominally equal for all samples the cycling performance under is remarkable different. Nearly one order of magnitude in cycling lifetime is observed for TBC systems under CMAS attack manufactured by Flame Spray on substrate material Rene 80 or Hastelloy X, respectively. For all systems an increase in cycling lifetime can be observed for deposits of reduced silica content (CMAF). At the same time the scatter of lifetime results among samples of the same type is remarkable increased.

Table 4: Summary of averaged cycling lifetime and predominant failure mode for the variants of state-of-the-art YSZ TBCs under attack from CMAS and CMAF deposits, respectively

Materials	Coating Manufacturer (BC/TBC)	CMAS		CMAF	
		Average Lifetime	Failure Mode	Average Lifetime	Failure Mode
Rene 80 / SC2464 / YSZ	FS / FZJ	158	shallow / deep	228	deep / shallow
Rene 80 / SC2464 / YSZ	FS / FS	177	deep	279	shallow
Rene 80 / SC2464 / YSZ	FZJ / FZJ	37	deep	337	deep
Hastelloy X / SC2231 / YSZ	FS / FS	24	shallow	337	shallow

Although resistance against CMAS type deposits seems to be more important to prevent rapid degradation on slag deposits a favorite coating system to withstand best any kind of deposit composition cannot be identified from the testing, yet. Porosity as well as thickness of the ceramic topcoat, roughness of the bondcoat, and thermo-mechanical properties of the substrate are apparently influencing cycling performance and failure modes. Further evaluation of results and studies seem to be necessary to deduce generalized advice for CMAS/F resistant coating microstructure. Results from on-going evaluation of samples after test will be summarized as part of deliverable D2.2.8.